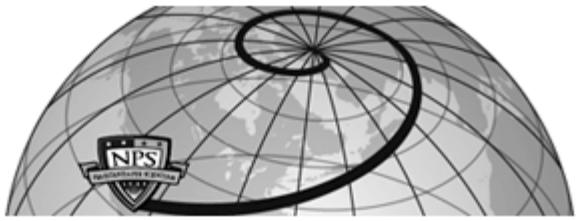

A FIVE-LEVEL BAROCLINIC PREDICTION MODEL.

CELIA L. BARTEAU AND
WILLIAM D. GROSCUP.

A FIVE-LEVEL BAROCLINIC PREDICTION MODEL

* * * * *

Celia L. Barteau

and

William D. Groscup

A FIVE-LEVEL BAROCLINIC PREDICTION MODEL

by

Celia L. Barteau

Lieutenant Commander, United States Navy

and

William D. Groscup

Lieutenant, United States Navy

Submitted in partial fulfillment of
the requirements for the degree of

MASTER OF SCIENCE
IN
METEOROLOGY

United States Naval Postgraduate School
Monterey, California

1 9 6 3

A FIVE-LEVEL BAROCLINIC PREDICTION MODEL

by

Celia L. Barteau

and

William D. Groscup

This work is accepted as fulfilling
the thesis requirements for the degree of
MASTER OF SCIENCE
IN
METEOROLOGY
from the
United States Naval Postgraduate School

ABSTRACT

A five-level baroclinic model for numerical prediction of height fields at 1000, 850, 700, 500, and 300 mb is developed and programmed. Several forms of the model are tested to determine the contribution of the various terms of the vorticity equation. Forecasts from three different methods are compared. The model shows utility in prognosis. Although there are individual differences among the methods, no one of the three is significantly better over the entire hemisphere on the data tested here.

The writers wish to express their appreciation to Professor George Haltiner of the U. S. Naval Postgraduate School for his assistance and guidance in this investigation. Appreciation is also expressed to the personnel of the U. S. Navy Fleet Numerical Weather Facility for their cooperation during the preparation of this paper. We are especially indebted to CDR L. C. Clarke and LT G. Lawniczak for use of their solution of the omega equation, and for their assistance to us, and to LCDR M. Jane Frawley for her aid and advice in programming.

TABLE OF CONTENTS

Table of Symbols

g	the upward component of the apparent gravitational acceleration
D	the altimeter correction $D = Z - Z_p$
Z	the height of an isobaric surface
Z_p	the pressure altitude in the standard atmosphere
f	the Coriolis parameter, $2\Omega \sin\phi$, where ϕ is the geographical latitude
$\bar{f}$	the mean value of the Coriolis parameter, $2\Omega \sin 45°$
Φ	the geopotential
ζ	the relative vorticity $\zeta = \frac{\partial v}{\partial x} - \frac{\partial u}{\partial y}$
η	the absolute vorticity $\eta = \zeta + f$
ψ	the stream function for the non-divergent component of velocity
χ	the velocity potential for the divergent component of velocity
ω	the vertical velocity of air in pressure coordinates
p	the atmospheric pressure in millibars
σ	the static stability $\sigma = -\frac{T}{\theta}\frac{\partial \theta}{\partial p}$
R	the universal gas constant
d	grid distance, 381 km at 60N
m	map scale factor
∇	del operator on a constant-pressure surface
∇^2	horizontal Laplacian operator on a constant-pressure surface
J	horizontal Jacobian operator $J(A,B) = \frac{\partial A}{\partial x}\frac{\partial B}{\partial y} - \frac{\partial A}{\partial y}\frac{\partial B}{\partial x}$
∇^2	finite difference Laplacian $\nabla^2 A = (A_{i+1,j} + A_{i,j+1} + A_{i-1,j} + A_{i,j-1} - 4A_{i,j})$
$\mathbb{J}$	finite difference Jacobian $\mathbb{J}(A,B) = \left[(A_{i+1,j} - A_{i-1,j})(B_{i,j+1} - B_{i,j-1}) - (A_{i,j+1} - A_{i,j-1})(B_{i+1,j} - B_{i-1,j})\right]$

1. Introduction.

Until very recently, the barotropic models have been the principal source of numerical weather prognoses. Their shortcomings in areas of baroclinic development, plus the advent of sophisticated digital computer systems, have spurred interest in baroclinic models. It is the purpose of this research to develop and program a five-level baroclinic model and to investigate the contribution of the various terms of the vorticity equation to the prognosis of the pressure field.

2. Background.

In the model developed here, prognosis is accomplished by means of the vorticity equation, which, with pressure as the vertical coordinate, can be written

$$\frac{\partial \zeta}{\partial t} = -J(\psi, \eta) - \left(\frac{\partial \chi}{\partial x}\frac{\partial \eta}{\partial x} + \frac{\partial \chi}{\partial y}\frac{\partial \eta}{\partial y}\right) + \eta\frac{\partial \omega}{\partial p} - \omega\frac{\partial \zeta}{\partial p} + \left(\frac{\partial \omega}{\partial y}\frac{\partial^2 \psi}{\partial x\,\partial p} - \frac{\partial \omega}{\partial x}\frac{\partial^2 \psi}{\partial y\,\partial p}\right). \qquad (1)$$

Basic to the derivation of this equation is the Helmholtz theorem which expresses the wind as the sum of a divergent and a non-divergent component:

$$\mathbb{V} = \mathbb{k} \times \nabla\psi + \nabla\chi. \qquad (2)$$

The potential function χ for the divergent part of the wind is obtained through solution of the continuity equation

$$\nabla^2\chi + \frac{\partial \omega}{\partial p} = 0. \qquad (3)$$

The stream function ψ for the non-divergent portion is approximated by solution of the balance equation

$$f\nabla^2\psi + 2\left[\frac{\partial^2 \psi}{\partial x^2}\cdot\frac{\partial^2 \psi}{\partial y^2} - \left(\frac{\partial^2 \psi}{\partial x\,\partial y}\right)\right] + \nabla f\cdot\nabla\psi - \nabla^2\Phi = 0 \qquad (4)$$

as described by G. 'Arnason [1], where Φ is the geopotential. Use of the stream function in the vorticity equation enables one to avoid the geostrophic approximation and the concomitant spurious anticyclogenesis.

The vertical component of relative vorticity, ζ, is the Laplacian of the stream function

$$\zeta = \nabla^2\psi \qquad (5)$$

and absolute vorticity, η, is the sum of this and the vertical component of the earth's vorticity, f.

$$\eta = \zeta + f \tag{6}$$

Vertical velocity, ω, is computed by the diagnostic equation

$$\nabla^2\omega + \frac{p\bar{f}^2}{\sigma R}\frac{\partial^2\omega}{\partial p^2} = \frac{g}{f}\left[\nabla^2 J(Z,T) - J(Z,\nabla^2 T) - \frac{f}{g}J(T,\eta)\right], \tag{7}$$

developed by Clarke and Lawniczak [3]. The forcing function is calculated with the geostrophic approximation. This results in some inconsistencies in the model but to avoid reprogramming the entire equation, we have gone ahead with comparison-type experiments. Vertical velocity is assumed zero at 100 mb, but other boundary conditions are among the options available to the user of this computer program as follows:

a) the lower boundary can be level or include terrain;

b) vertical velocity can be set equal to zero at the lower boundary, or computed with or without terrain effects and with or without the effect of friction;

c) the stability parameter σ can be a point variable, a function of pressure alone, or a constant; and

d) the maximum acceptable residual in the 3-dimensional relaxation can be selected by the user.

In the vorticity equation, the contributions from the twisting term, $\left(\frac{\partial\omega}{\partial x}\frac{\partial^2\psi}{\partial x\,\partial p} - \frac{\partial\omega}{\partial y}\frac{\partial^2\psi}{\partial y\,\partial p}\right)$, and the vertical advection of vorticity term, $\omega\frac{\partial\zeta}{\partial p}$, are usually considered small, and some investigations have shown that they tend to compensate each other [2]. Also, integral theorems show [4] that to avoid the mean generation of vorticity in a closed

volume, the two terms should be included or neglected together. Both have been omitted from the initial investigation reported here.

A further simplification involves omission of the advection of absolute vorticity by the divergent portion of the wind, $\frac{\partial \chi}{\partial x}\frac{\partial \eta}{\partial x} + \frac{\partial \chi}{\partial y}\frac{\partial \eta}{\partial y}$. For consistency, it is necessary then also to substitute the mean value of the Coriolis parameter, $\bar{f}$, for the absolute vorticity in the divergence term, $\bar{f}\frac{\partial \omega}{\partial p}$.

In the equations that follow, the stream function has been redefined so as to be in units of height,

$$\psi = \frac{g}{\bar{f}} E . \tag{8}$$

The resulting forms of the vorticity equation, expressed in finite-difference notation, are

$$\frac{m^2 g}{d^2 \bar{f}} \nabla^2 \frac{\Delta E}{\Delta t} = \frac{-g m^2}{\bar{f} 4 d^2} \mathcal{J}(E, \eta) + \bar{f} \frac{\Delta \omega}{\Delta p}, \tag{9}$$

$$\frac{m^2 g}{d^2 \bar{f}} \nabla^2 \frac{\Delta E}{\Delta t} = \frac{-g m^2}{\bar{f} 4 d^2} \mathcal{J}(E, \eta) - \frac{g m^2}{\bar{f} 4} \left(\frac{\Delta \chi}{\Delta x}\frac{\Delta \eta}{\Delta x} + \frac{\Delta \chi}{\Delta y}\frac{\Delta \eta}{\Delta y} \right) + \eta \frac{\Delta \omega}{\Delta p}, \tag{10}$$

and the complete equation

$$\frac{m^2 g}{d^2 \bar{f}} \nabla^2 \frac{\Delta E}{\Delta t} = \frac{-g m^2}{\bar{f} 4 d^2} \mathcal{J}(E, \eta) - \frac{g m^2}{\bar{f} 4} \left(\frac{\Delta \chi}{\Delta x}\frac{\Delta \eta}{\Delta x} + \frac{\Delta \chi}{\Delta y}\frac{\Delta \eta}{\Delta y} \right) + \eta \frac{\Delta \omega}{\Delta p}$$

$$- \frac{g m^2}{\bar{f} d^2} \omega \nabla^2 \frac{\Delta E}{\Delta p} + \frac{g m^2}{\bar{f} 4} \left(\frac{\Delta \omega}{\Delta y}\frac{\Delta^2 E}{\Delta y \Delta p} - \frac{\Delta \omega}{\Delta x}\frac{\Delta^2 E}{\Delta x \Delta p} \right), \tag{11}$$

where d is the grid distance and m is the ratio of this distance to the corresponding geographical distance.

Horizontal spatial operators are approximated by the usual centered differences. To approximate the vertical derivatives in the vorticity equation a Lagrangian parabola was fitted through three points. For a centered difference the equation is

$$\left(\frac{\Delta A}{\Delta P}\right)_{p=p_1} \doteq \frac{(p_1-p_2)}{(p_0-p_1)(p_0-p_2)}A_0 + \frac{(2p_1-p_0-p_2)}{(p_1-p_0)(p_1-p_2)}A_1 + \frac{(p_1-p_0)}{(p_2-p_0)(p_2-p_1)}A_2 \quad . \tag{12}$$

All computations were done on the Control Data Corporation model 1604 computer, using the U. S. Navy Fleet Numerical Weather Facility octagonal grid. This grid, centered at the pole and inscribed in the 10N latitude circle, consists of 1977 grid points with a grid size of 381 km at 60N.

The week of 22 November 1962 was a period of considerable cyclogenesis in dense-data areas, and therefore excellent for testing a baroclinic model. Initial data used were the U. S. Navy Fleet Numerical Weather Facility height analyses at 1000, 850, 700, 500, and 300 mb for 1200Z on 22 November 1962. The height analyses for 0000Z and 1200Z 23 November were used in the evaluation of the predictions.

3. Procedures.

In the diagnostic ω-equation for the initial tests discussed here, the boundary conditions used are:

a) vertical velocity equal to zero at 100 mb;

b) vertical velocity equal to zero at the lower boundary;

c) no terrain effects at the lower boundary; and

d) the stability parameter, σ , is a function of pressure. The program is used in "forecast mode"; that is, temperatures are computed hydrostatically, rather than taken from objective analysis. The maximum residual in the 3-dimensional relaxation is 1×10^{-4} mb per second.

The sequence of calculations programmed can best be explained with reference to figure 1. Input data in every case are the U. S. Navy Fleet Numerical Weather Facility height analyses at the five standard levels, modified to ensure vertical consistency.

In the first method with equation (9), stream functions are used throughout. The inversion to height fields [1], effectively the reverse of the balance equation, is thus bypassed and stream functions are used for input data for both diagnostic and prognostic equation. This is hereafter referred to as method I. The resulting 24-hour prognoses are displayed on charts 6 through 10 and discussed in section 4 below.

Since the geostrophic approximation is used in the forcing function of the ω-equation, and temperatures are computed hydrostatically, there might be some reason to suspect the vertical velocities computed from height fields could be more accurate than those from stream functions. A completely geostrophic model was programmed, using pressure-height data throughout. This method showed the expected spurious anticyclogenesis even at 12 hours and was carried no further.

The complete process diagrammed in figure 1 has been used in the remainder of this investigation. In the first time step the initial data (five vertically-consistent height fields) are used as input to the balance equation and to the ω-equation. From the former are obtained stream functions for the five levels; the latter yields vertical velocities at the same levels. With these stream functions and vertical velocities the vorticity equation (equation (9) for method II, equation (10) for method III) gives $\frac{\Delta E}{\Delta t}$, the local change in stream function, at the five levels. When these are added to the initial values, the first forecast time step is complete. As shown in figure 1, these new E values are now input fields for both the vorticity equation and the balance equation; the latter being used for inversion to pressure height as required by the ω-equation.

Subsequent time steps follow the same routine, except in the application of $\frac{\Delta E}{\Delta t}$, which is done according to the centered-difference equation

$$E_{k-1} + 2\left(\frac{\Delta E}{\Delta t}\right)_{k-1} \Delta t = E_{k+1} \quad . \tag{13}$$

In order to minimize the errors inherent in the initial forward time step, the first time increment is only 15 minutes. Centered time steps are then used to complete successive 15-minute prognoses to one hour, and finally 1-hour prognoses to 12 hours. The fields are then smoothed lightly to remove any small perturbations resulting from truncation or round-off errors, and the process is repeated to 24 hours.

4. Results.

In review: method I uses stream functions throughout, and with equation (9) as the prognostic equation excludes the advection of absolute vorticity by the divergent portion of the wind and substitutes $\bar{f}$ for η in the divergence term; method II inverts the stream-function fields to pressure heights at every time step, but retains the other simplifications of method I; method III also inverts to pressure height at each time step, but uses the more complete equation (10) as the prognostic equation.

Charts 1-5 are the pressure height analyses at the beginning of the period. The next 15 charts are the results of the three 24-hour forecasts: method I in charts 6-10; method II, charts 11-15; and method III, charts 16-20. Charts 21-25 are the observed height analyses at the end of the forecast period. Chart 26 is the U. S. Navy Fleet Numerical Weather Facility barotropic forecast at 500 mb for the same period. Table 1 shows the contour origin and interval for all the charts.

In general, corresponding charts from the three methods are quite similar. They all retain a typical meteorological appearance and the various systems show a reasonable vertical structure. Further indication of their similarity is contained in table 2. The "pillow" referred to is

$$\text{Pillow} = \frac{\sum_{m=1}^{1977} (A-B)_m}{1977} \tag{16}$$

and the RMSE is the root-mean-square error calculated in the usual fashion:

$$\text{RMSE} = \sqrt{\frac{\sum_{m=1}^{m=1977} \left[(A-B)-\text{Pillow} \right]_m^2}{1977}} \quad . \qquad (17)$$

Nevertheless, a level-by-level comparison of the three forecast methods shows some differences among them. At 1000 mb, for instance, the two low centers over North America merged and deepened, while the trough moved nearly 20° east. All methods forecast the merging and considerable trough movement, with method I giving the best placement of the trough. During the forecast period a low center developed in the area of weak gradient southwest of the Kamchatka peninsula. This development was forecast by all methods, although with too much cyclogenesis. Method I was again the best. In no case is there any evidence of spurious anticyclogenesis, even at low latitudes.

The forecasts at 850 and 700 mb show movement consistent with that forecast at 1000 mb. By 700 mb the tilt of the baroclinic systems has become apparent. A good example is the stationary low center over the Northwest Territories, which deepened by 26 meters. All forecasts held it stationary, but methods I and III forecast two and seven meters deepening, respectively, while method II forecast a 2-meter filling. The weakening of the low center east of Greenland was forecast by all methods, but best by method II.

At 500 mb, since the chart of the U. S. Navy Fleet Numerical Weather Facility barotropic forecast has been included, there are four charts to compare. There is a striking similarity between the barotropic prognosis and that from method I. The method II and III prognoses, themselves much alike, are quite different from the other two. Method I and the

USNFNWF model both forecast the movement and reorientation of the trough over Eastern United States, and the weakening and displacement of the low center near Hudson Bay. Methods II and III show the trough lagging far behind its true position, and retain the low as a stationary system. Method III even deepened it slightly. In contrast, methods II and III produced much better forecasts than the others in the western Europe-Mediterranean area.

At 300 mb all three methods agree in general on the movement and development of the major systems. This development is in some cases out of phase with the actual development, but no one method can be selected as better than the rest. The initial and verifying charts at 300 mb show more effect from the process of making the data vertically consistent than was evident at lower levels.

Referring again to table 2, there seems to be no best method among the three tested. Certainly the addition of the advection of absolute vorticity by the divergent wind and the use of absolute vorticity in the divergence term produced little change and no over-all improvement in this particular forecast. The effect of the inclusion of the vertical advection of absolute vorticity and the twisting term remains to be tested.

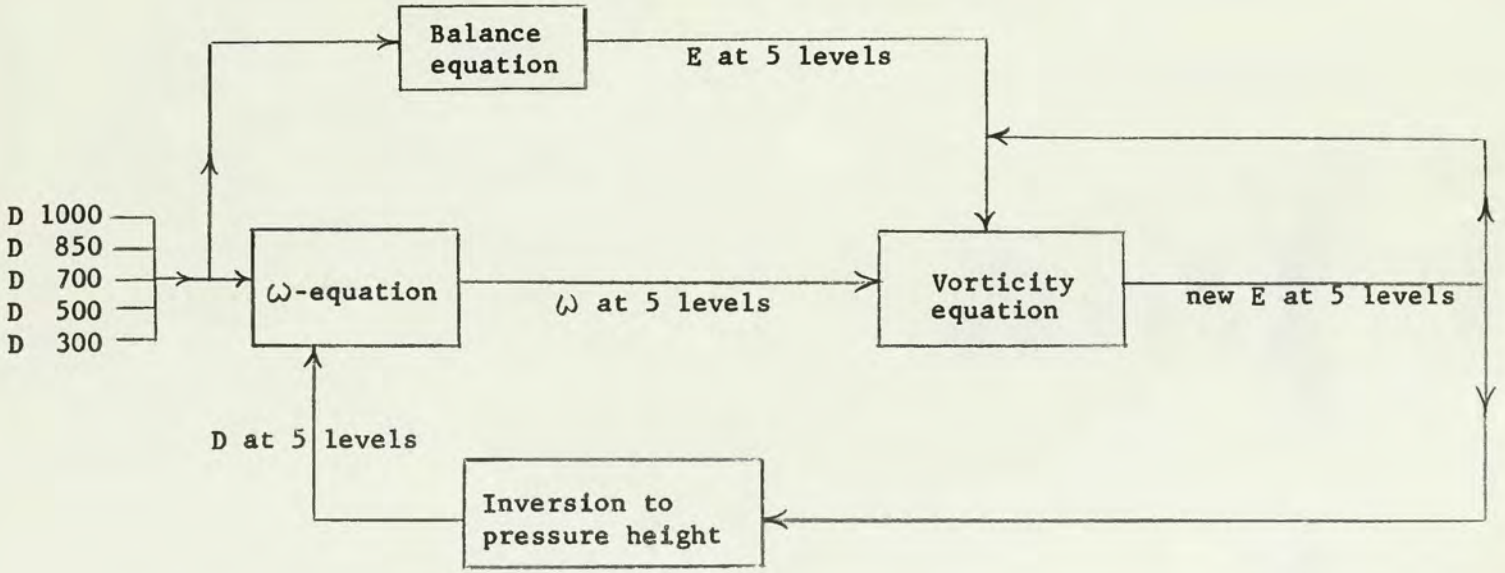
Balance equation
E at 5 levels
D 1000
D 850
D 700
D 500
D 300
ω-equation
ω at 5 levels
Vorticity equation
new E at 5 levels
D at 5 levels
Inversion to pressure height

Figure 1

Table 1

Level (mb)	Contour origin (meters)	Contour interval (meters)
1000	120	60
850	1440	60
700	3060	60
500	5580	60
300	9120	120

Table 2

Method	Level (mb)	Pillow (meters)	RMSE (meters)
I	1000	- 7.9	43.6
	850	- 1.8	37.6
	700	- 1.8	41.8
	500	- 1.2	51.3
	300	13.4	80.3
II	1000	-11.3	43.3
	850	- 2.7	40.8
	700	0	42.7
	500	- .6	53.4
	300	11.9	77.3
III	1000	- 9.1	49.1
	850	- 3.4	43.0
	700	- 2.4	43.6
	500	- 1.5	54.4
	300	13.4	80.0
USNFNWF	500	- 4.9	47.0
Persistence	500	- 3.3	57.4

BIBLIOGRAPHY

1. 'Arnason, G., A convergent method for solving the balance equation, J. of Meteor., 15 (2), pp 220-225, April, 1958.

2. 'Arnason, G., and L. Carstensen, The effects of vertical vorticity advection and the turning of vortex tubes in hemispheric forecasts with a two-level model, Monthly Weather Review 87 (4), pp 119-127, April, 1959.

3. Clarke, L. C., and G. E. Lawniczak Jr., Hemispheric solution of the omega equation including terrain and surface frictional effects, M.S. thesis, U. S. Naval Postgraduate School, Monterey, Calif., 1962.

4. Lorenz, E. N., Energy and numerical weather prediction, Tellus, 22 (4), pp 364-375, November, 1960.

APPENDIX I

The following charts were computed during the course of this study. They are included here for easy reference.

Charts 1 - 5	Analyses, 12Z 22 Nov 1962
Charts 6-10	24-hour prognoses, method I
Charts 11-15	24-hour prognoses, method II
Charts 16-20	24-hour prognoses, method III
Charts 21-25	Analyses, 12Z 23 Nov 1962
Chart 26	24-hour prognosis, USNFNWF

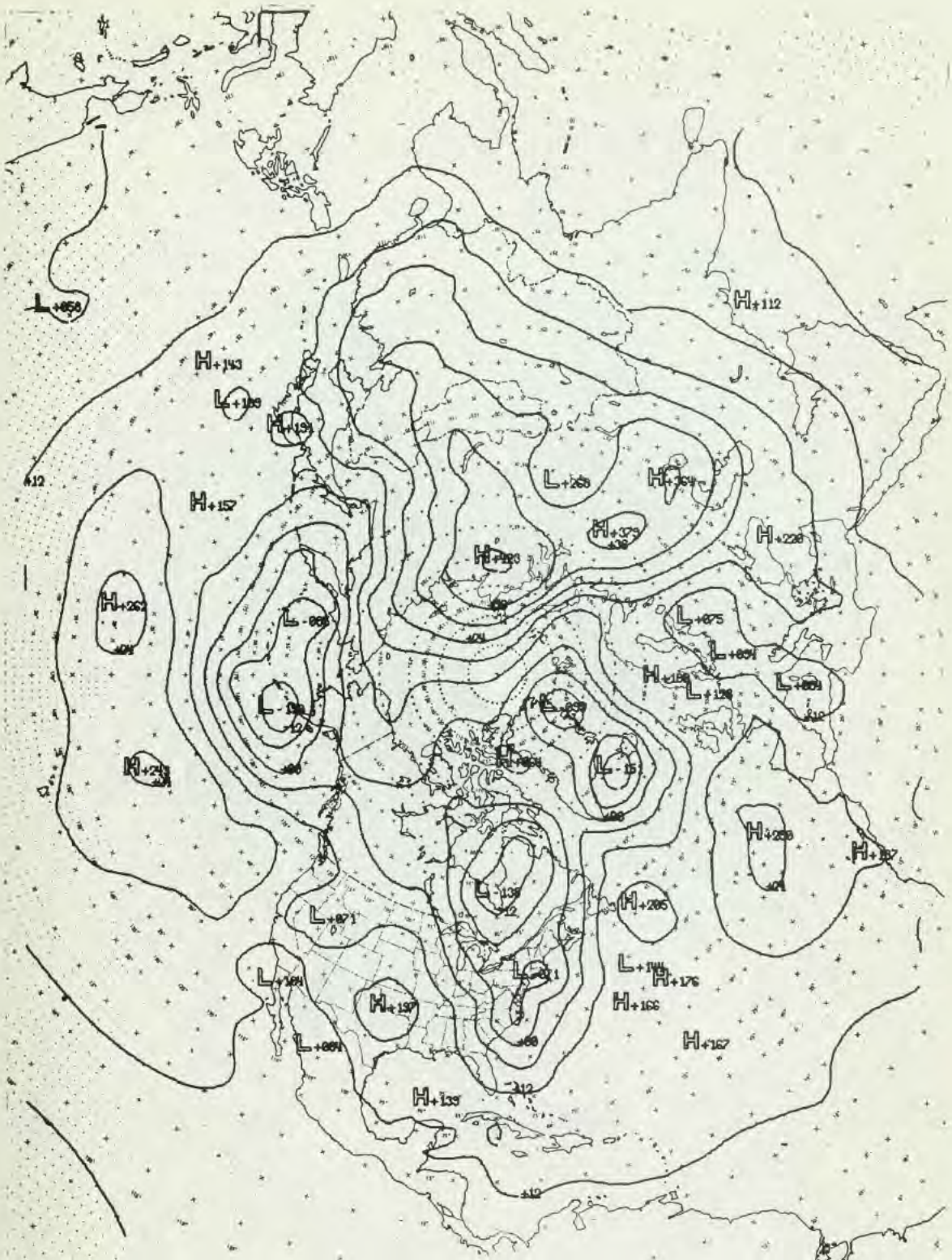
1000 HT ANAL 12Z 22 NOV 62 CHART 1
PROJECTION: POLAR STEREOGRAPHIC–TRUE AT 60° NORTH LATITUDE
SCALE 1:60,000,000
FLEET NUMERICAL WEATHER FACILITY
MONTEREY, CALIFORNIA
CHART NO. 6-B

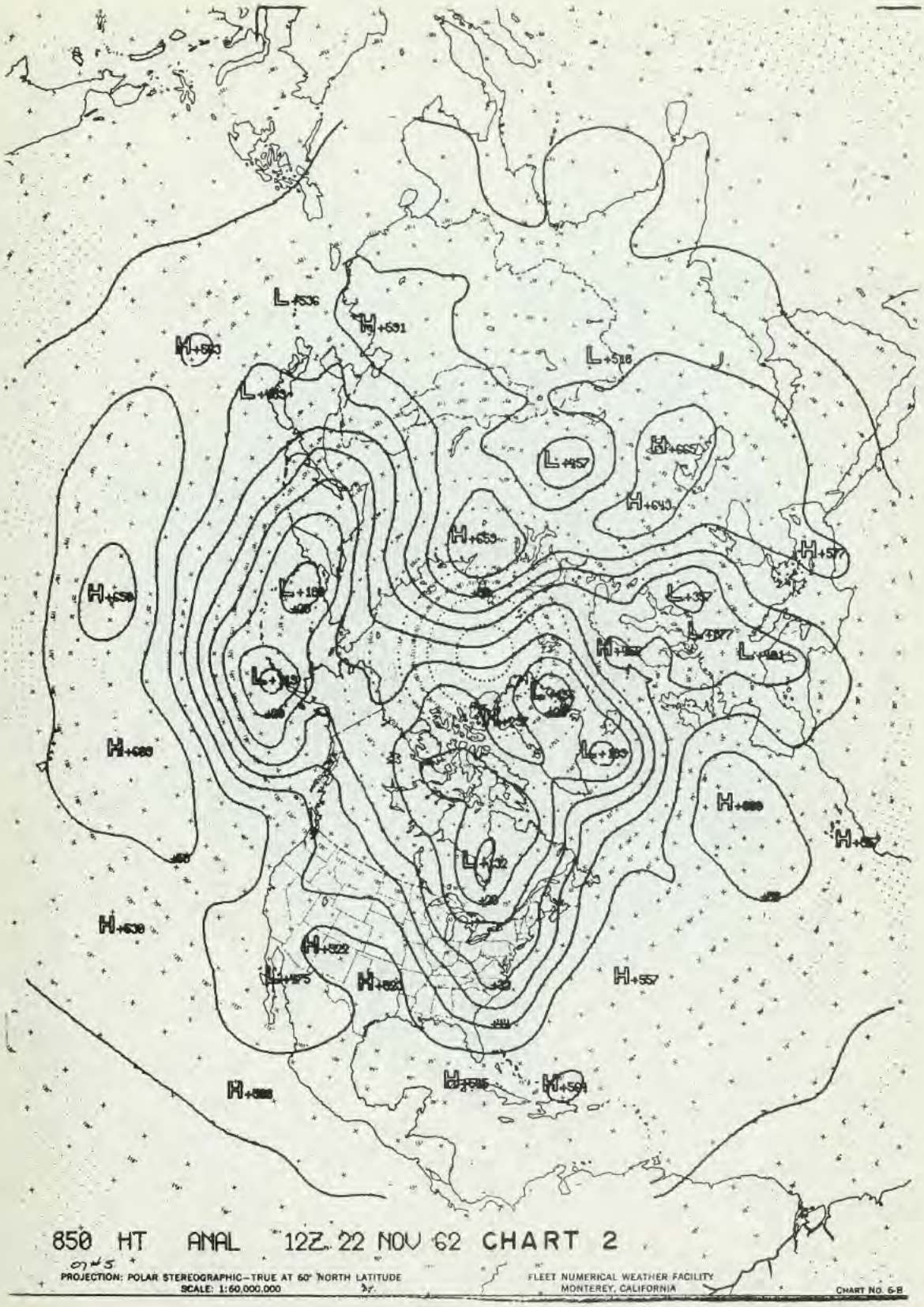
850 HT ANAL 12Z 22 NOV 62 CHART 2
PROJECTION: POLAR STEREOGRAPHIC—TRUE AT 60° NORTH LATITUDE
SCALE: 1:60,000,000
FLEET NUMERICAL WEATHER FACILITY
MONTEREY, CALIFORNIA
CHART NO. 6-8

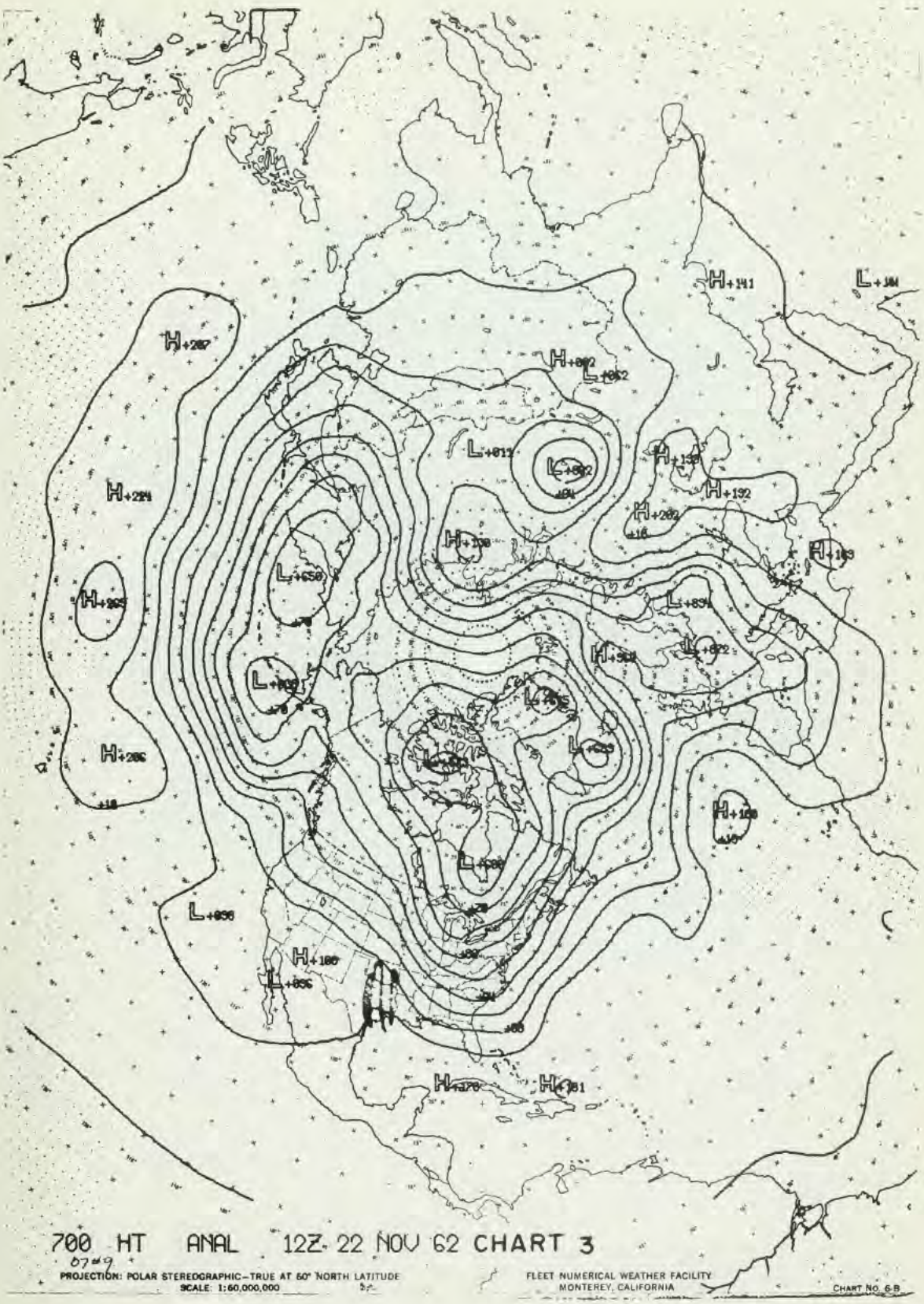
700 HT ANAL 12Z 22 NOV 62 CHART 3
0709
PROJECTION: POLAR STEREOGRAPHIC–TRUE AT 60° NORTH LATITUDE
SCALE: 1:60,000,000
FLEET NUMERICAL WEATHER FACILITY
MONTEREY, CALIFORNIA
CHART NO. 6-B

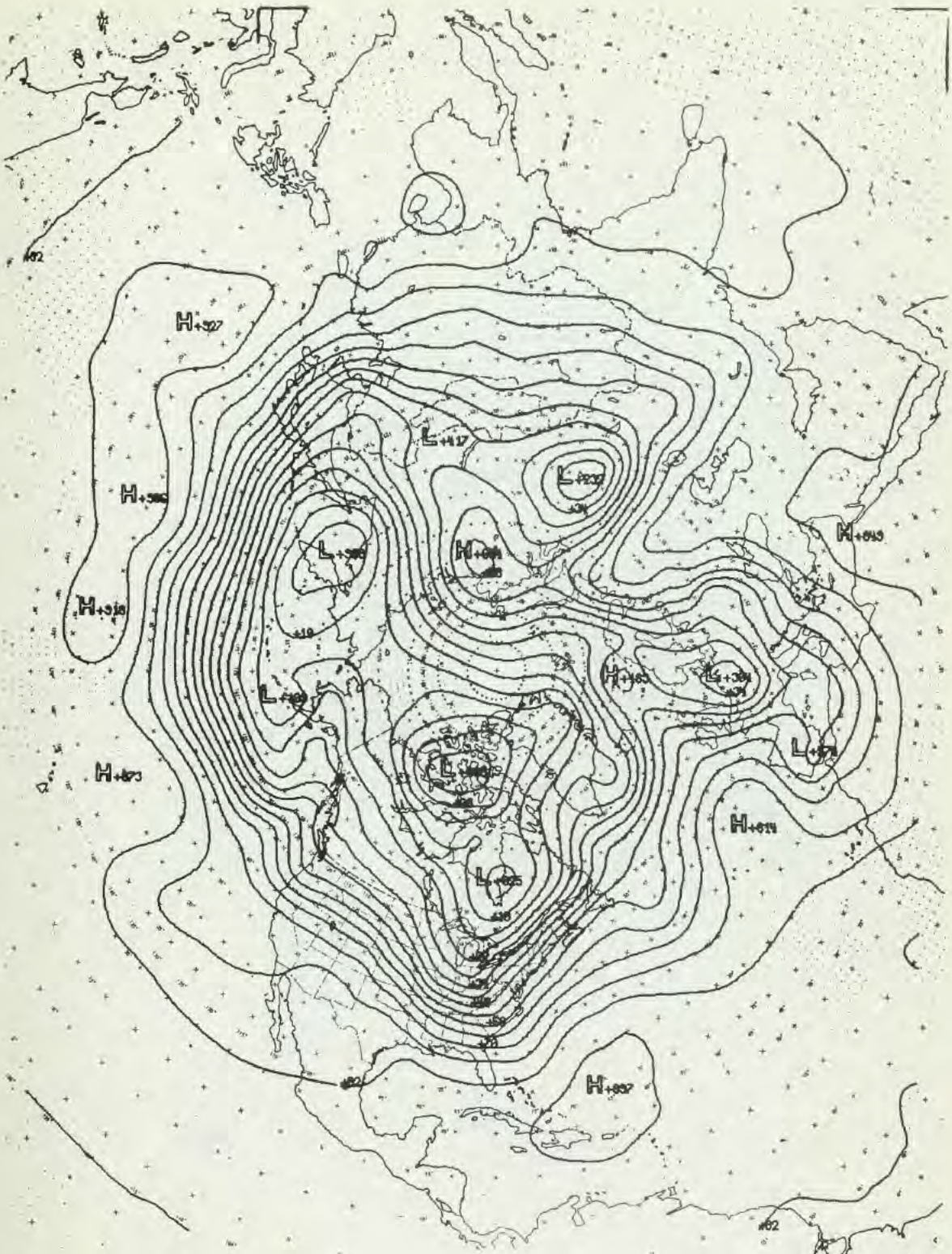
500 HT ANAL 12Z 22 NOV 62 CHART 4
PROJECTION: POLAR STEREOGRAPHIC—TRUE AT 60° NORTH LATITUDE
SCALE: 1:60,000,000
FLEET NUMERICAL WEATHER FACILITY
MONTEREY, CALIFORNIA
CHART NO. 6-8

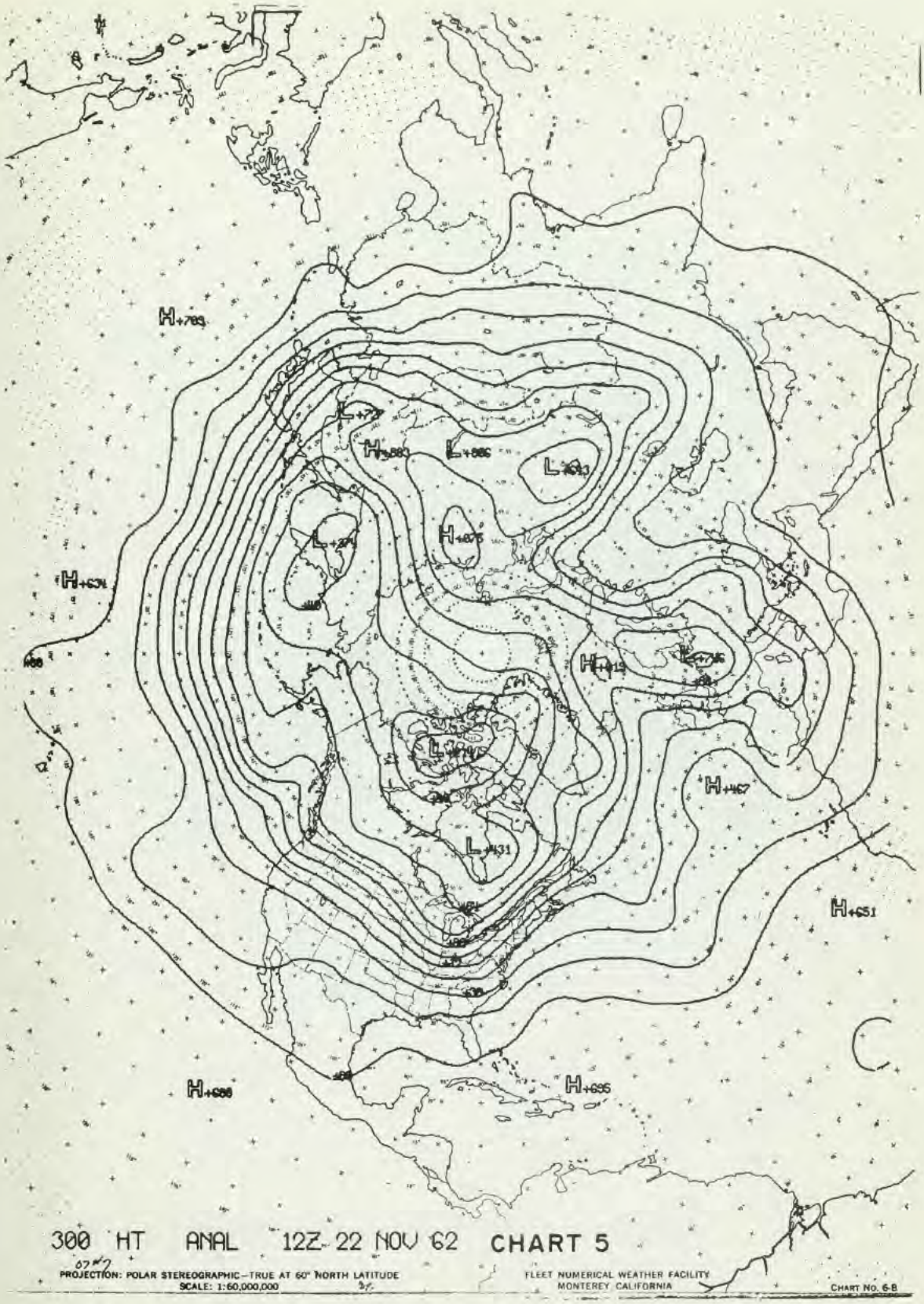
300 HT ANAL 12Z 22 NOV 62 CHART 5
PROJECTION: POLAR STEREOGRAPHIC—TRUE AT 60° NORTH LATITUDE
SCALE: 1:60,000,000
FLEET NUMERICAL WEATHER FACILITY
MONTEREY, CALIFORNIA
CHART NO. 6-8

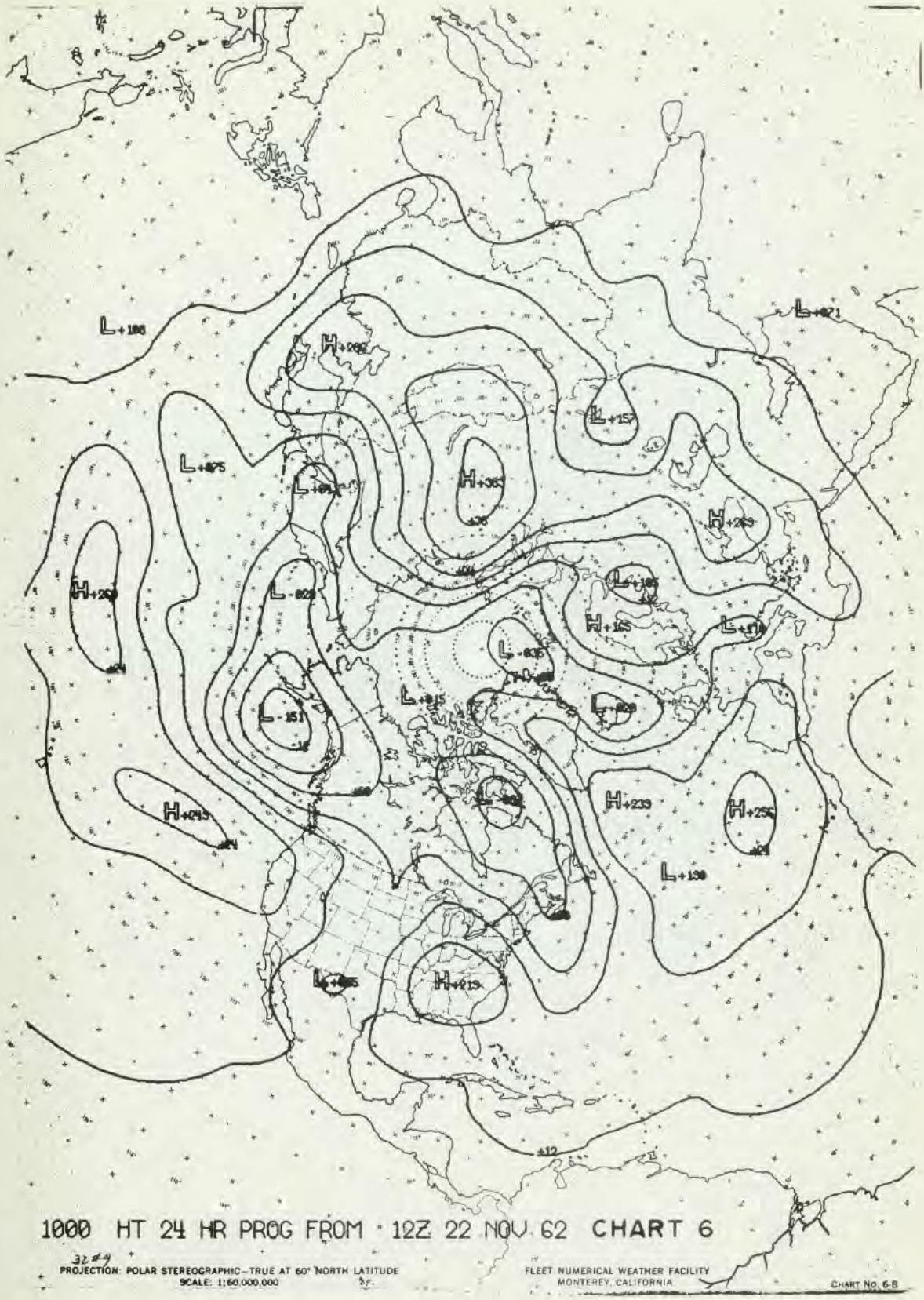
1000 HT 24 HR PROG FROM 12Z 22 NOV 62 CHART 6
PROJECTION: POLAR STEREOGRAPHIC – TRUE AT 60° NORTH LATITUDE
SCALE: 1:60,000,000
FLEET NUMERICAL WEATHER FACILITY
MONTEREY, CALIFORNIA
CHART NO. 6-8

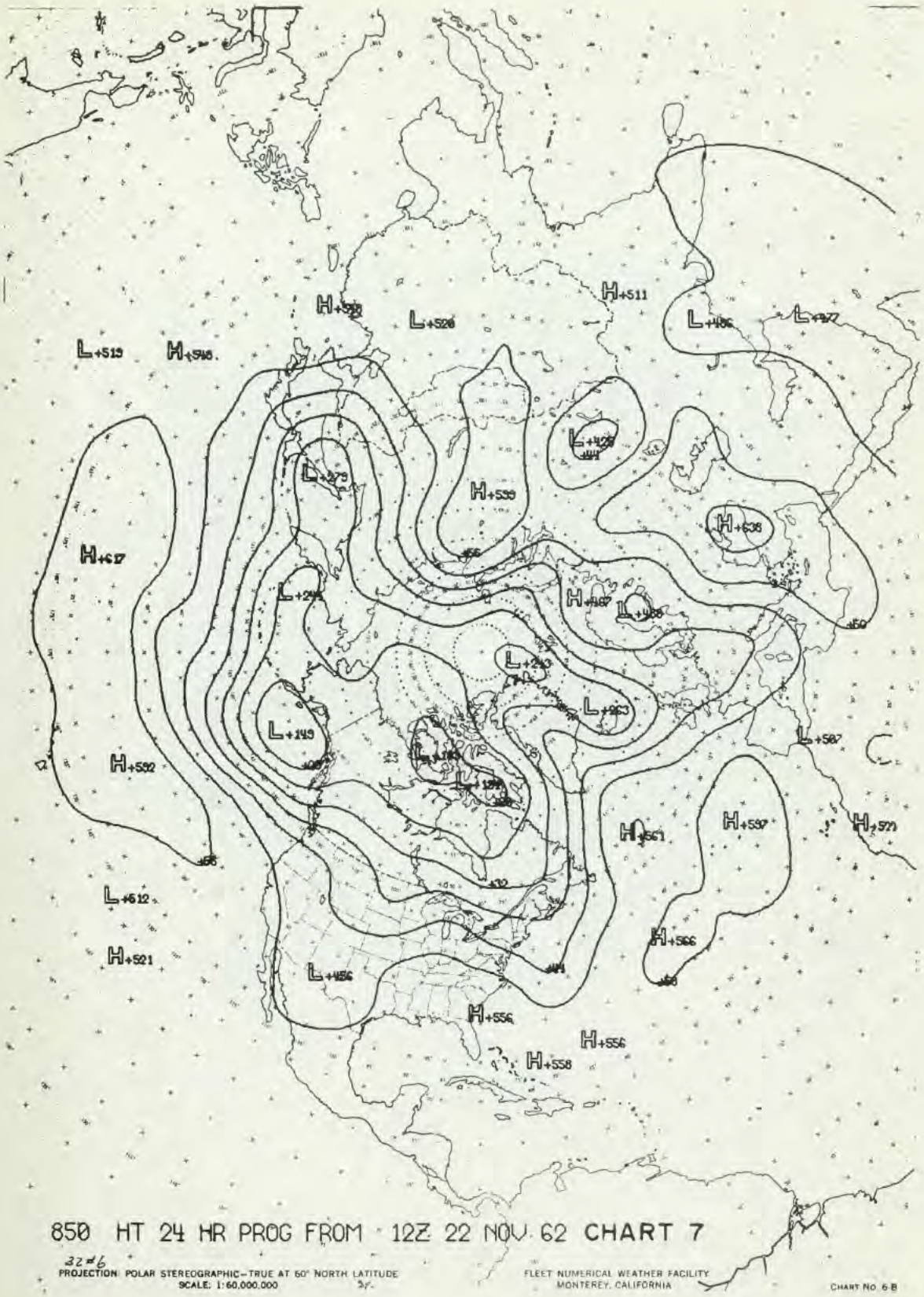

850 HT 24 HR PROG FROM 12Z 22 NOV 62 CHART 7

32N6

PROJECTION: POLAR STEREOGRAPHIC—TRUE AT 60° NORTH LATITUDE
SCALE: 1:60,000,000

FLEET NUMERICAL WEATHER FACILITY
MONTEREY, CALIFORNIA

CHART NO. 6-8

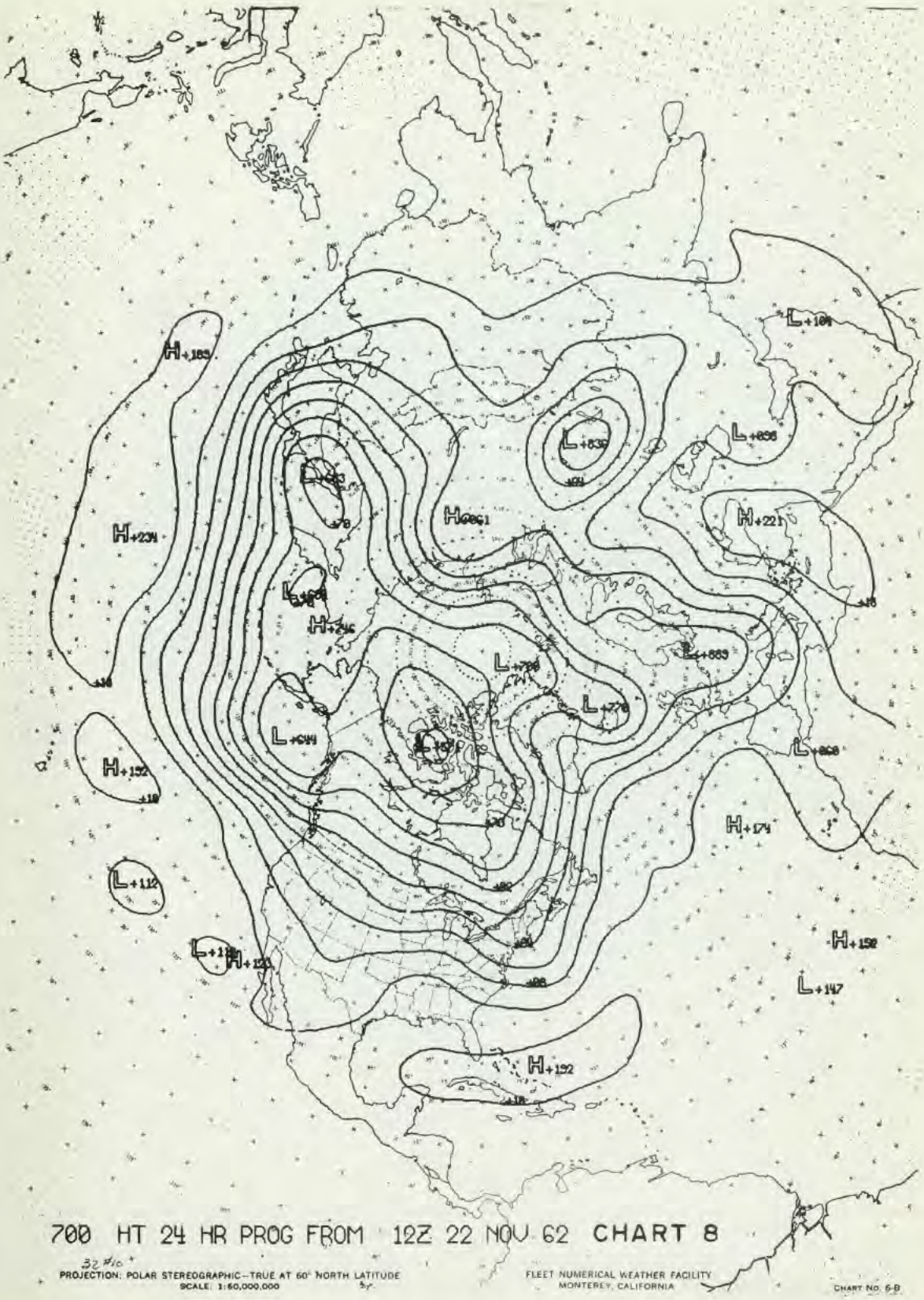

700 HT 24 HR PROG FROM 12Z 22 NOV 62 CHART 8

32 #10

PROJECTION: POLAR STEREOGRAPHIC—TRUE AT 60° NORTH LATITUDE
SCALE: 1:60,000,000

FLEET NUMERICAL WEATHER FACILITY
MONTEREY, CALIFORNIA

CHART NO. 6-8

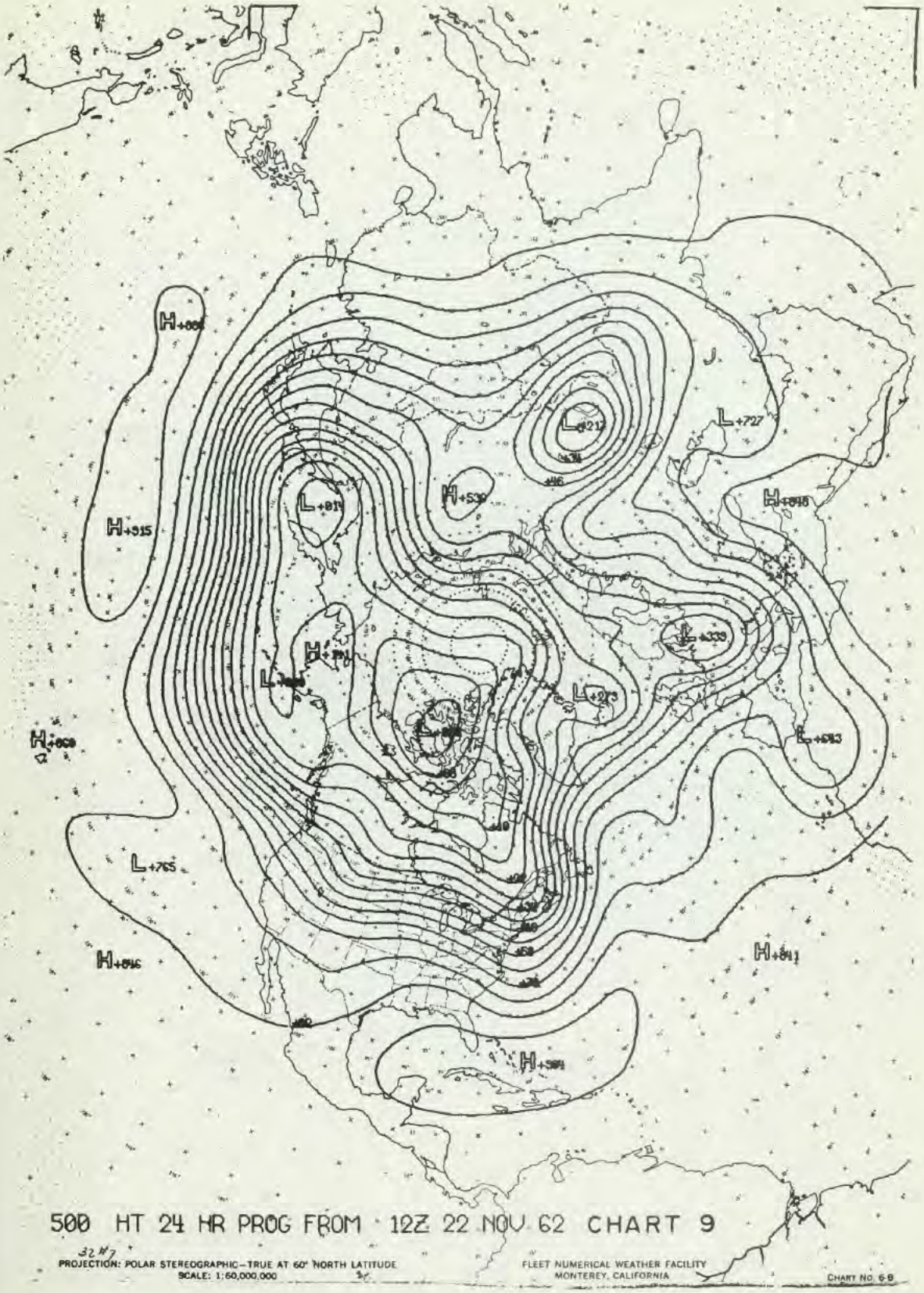
500 HT 24 HR PROG FROM 12Z 22 NOV 62 CHART 9
PROJECTION: POLAR STEREOGRAPHIC—TRUE AT 60° NORTH LATITUDE
SCALE: 1:60,000,000
FLEET NUMERICAL WEATHER FACILITY
MONTEREY, CALIFORNIA
CHART NO. 6-8

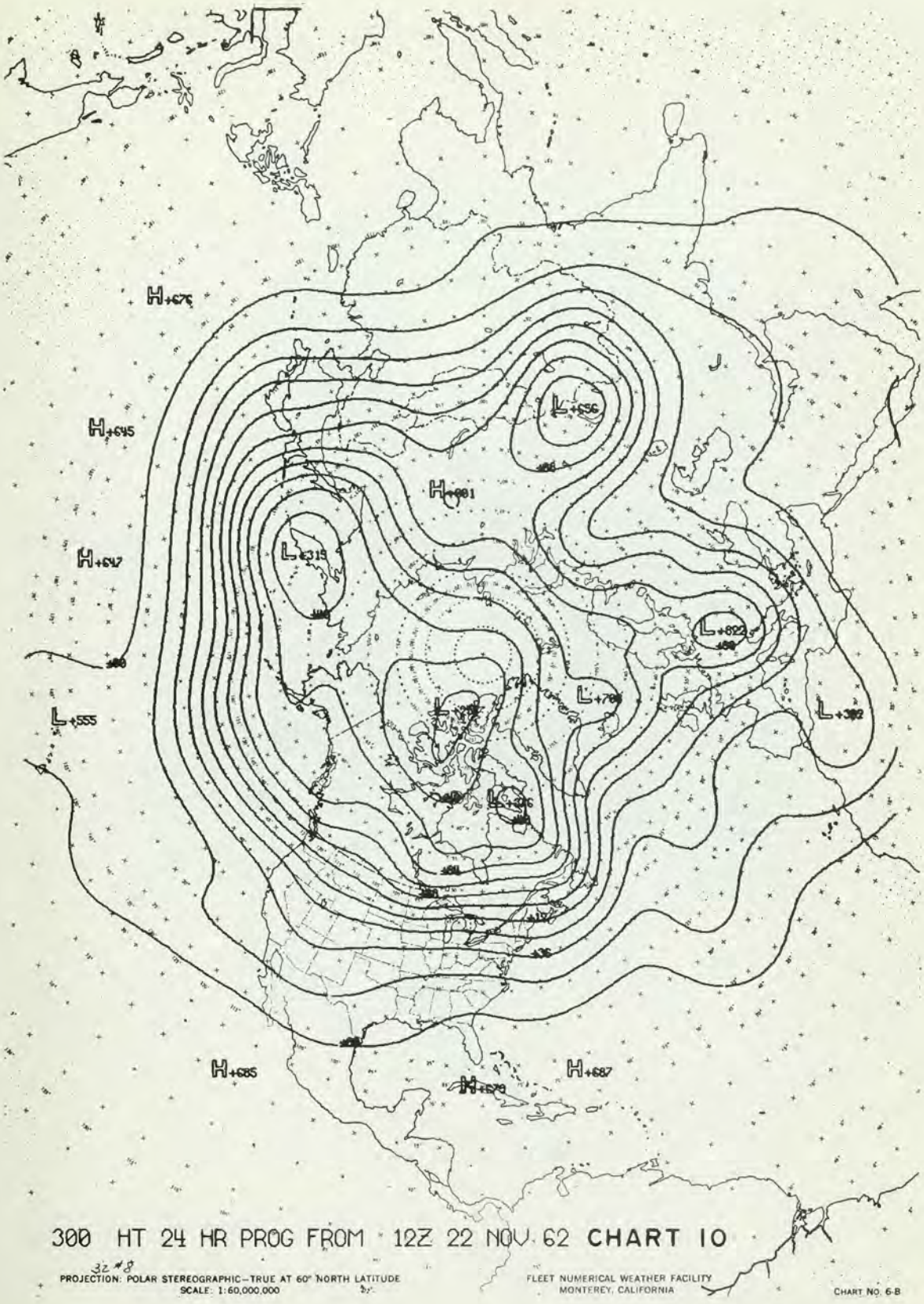

300 HT 24 HR PROG FROM 12Z 22 NOV 62 **CHART 10**

PROJECTION: POLAR STEREOGRAPHIC – TRUE AT 60° NORTH LATITUDE
SCALE: 1:60,000,000

FLEET NUMERICAL WEATHER FACILITY
MONTEREY, CALIFORNIA

CHART NO. 6-B

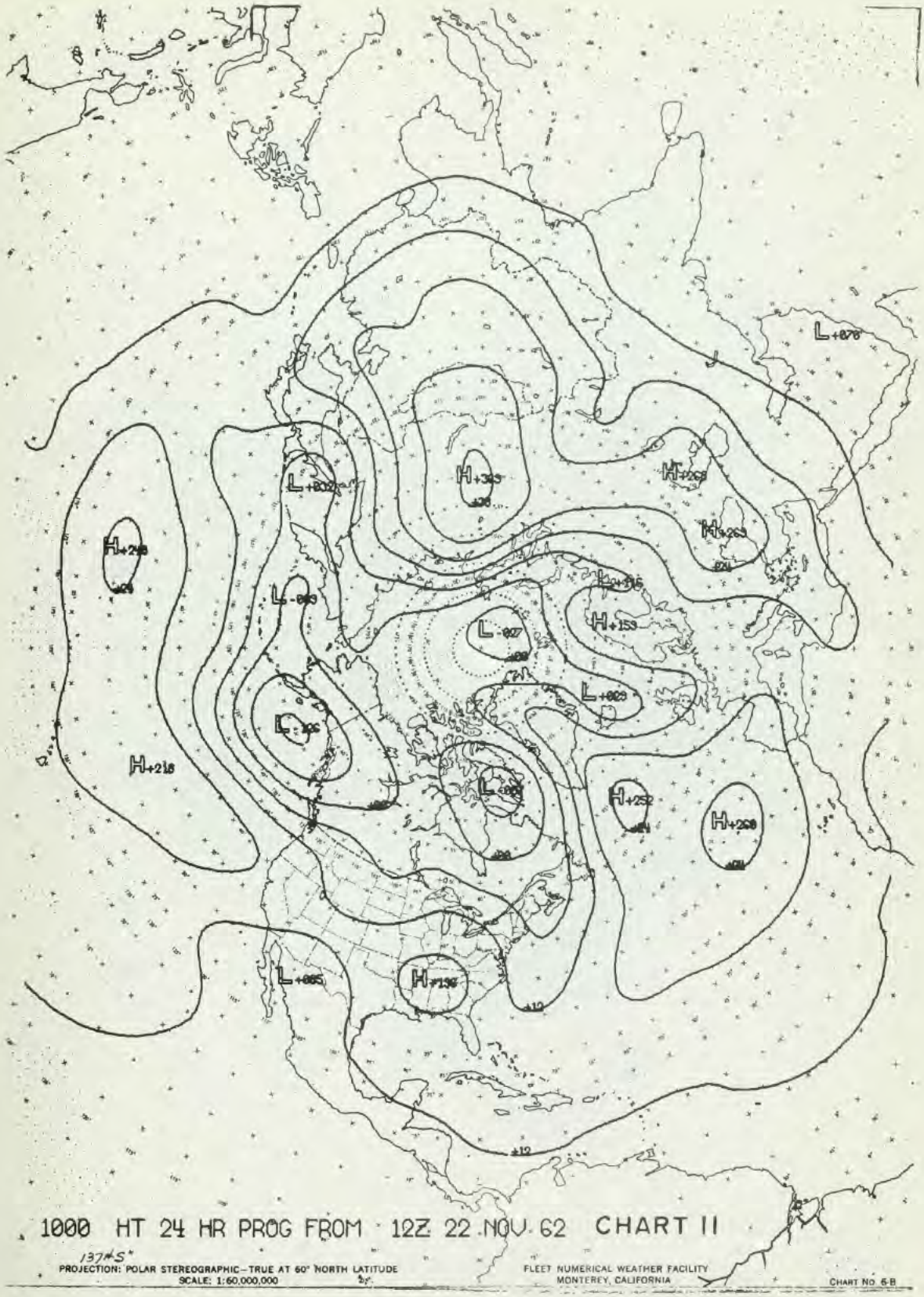

1000 HT 24 HR PROG FROM 12Z 22 NOV 62 CHART II

137#S*

PROJECTION: POLAR STEREOGRAPHIC—TRUE AT 60° NORTH LATITUDE
SCALE: 1:60,000,000

FLEET NUMERICAL WEATHER FACILITY
MONTEREY, CALIFORNIA

CHART NO. 6-B

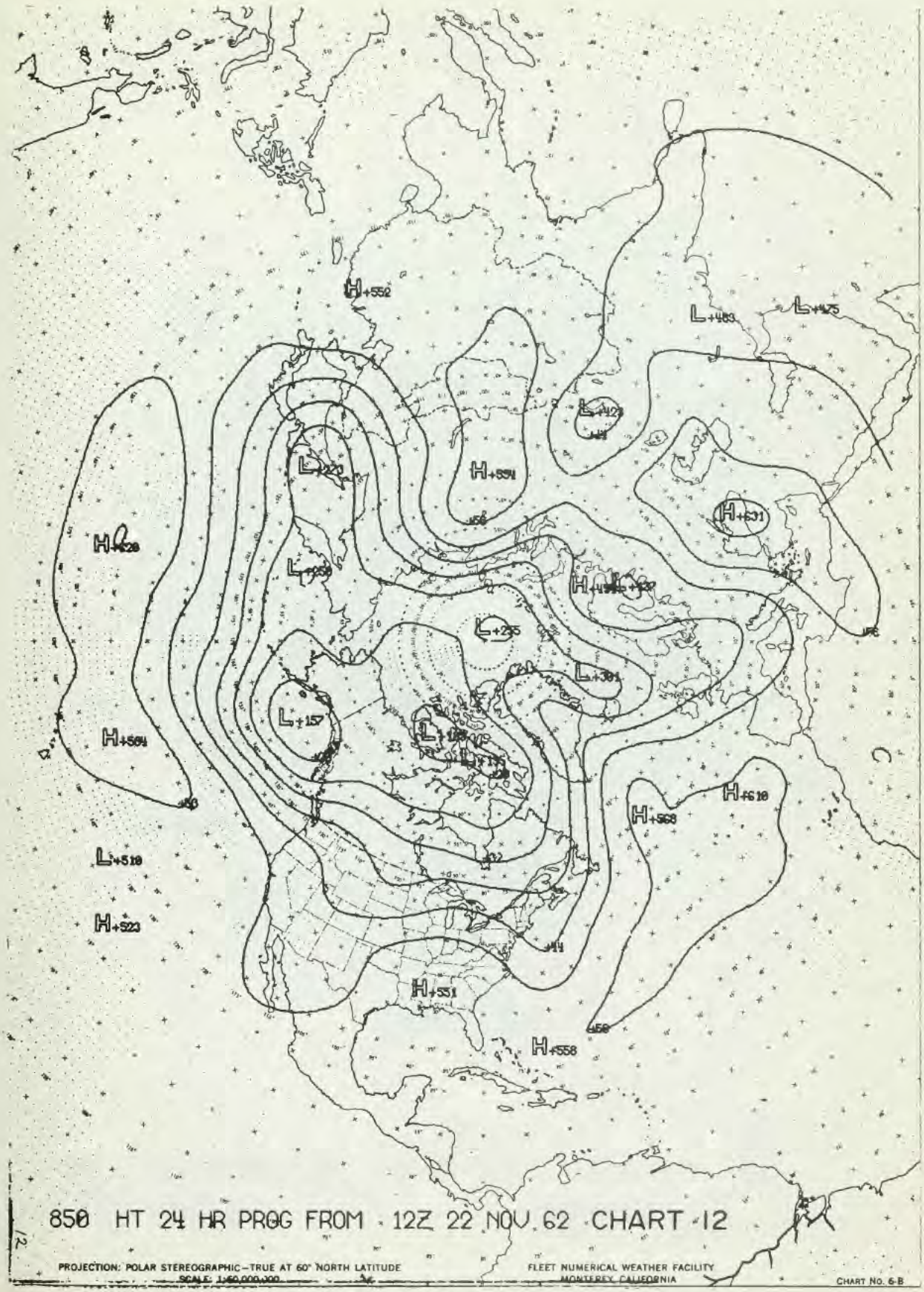

850 HT 24 HR PROG FROM 12Z 22 NOV 62 CHART 12

PROJECTION: POLAR STEREOGRAPHIC—TRUE AT 60° NORTH LATITUDE
SCALE: 1:60,000,000

FLEET NUMERICAL WEATHER FACILITY
MONTEREY, CALIFORNIA

CHART NO. 6-B

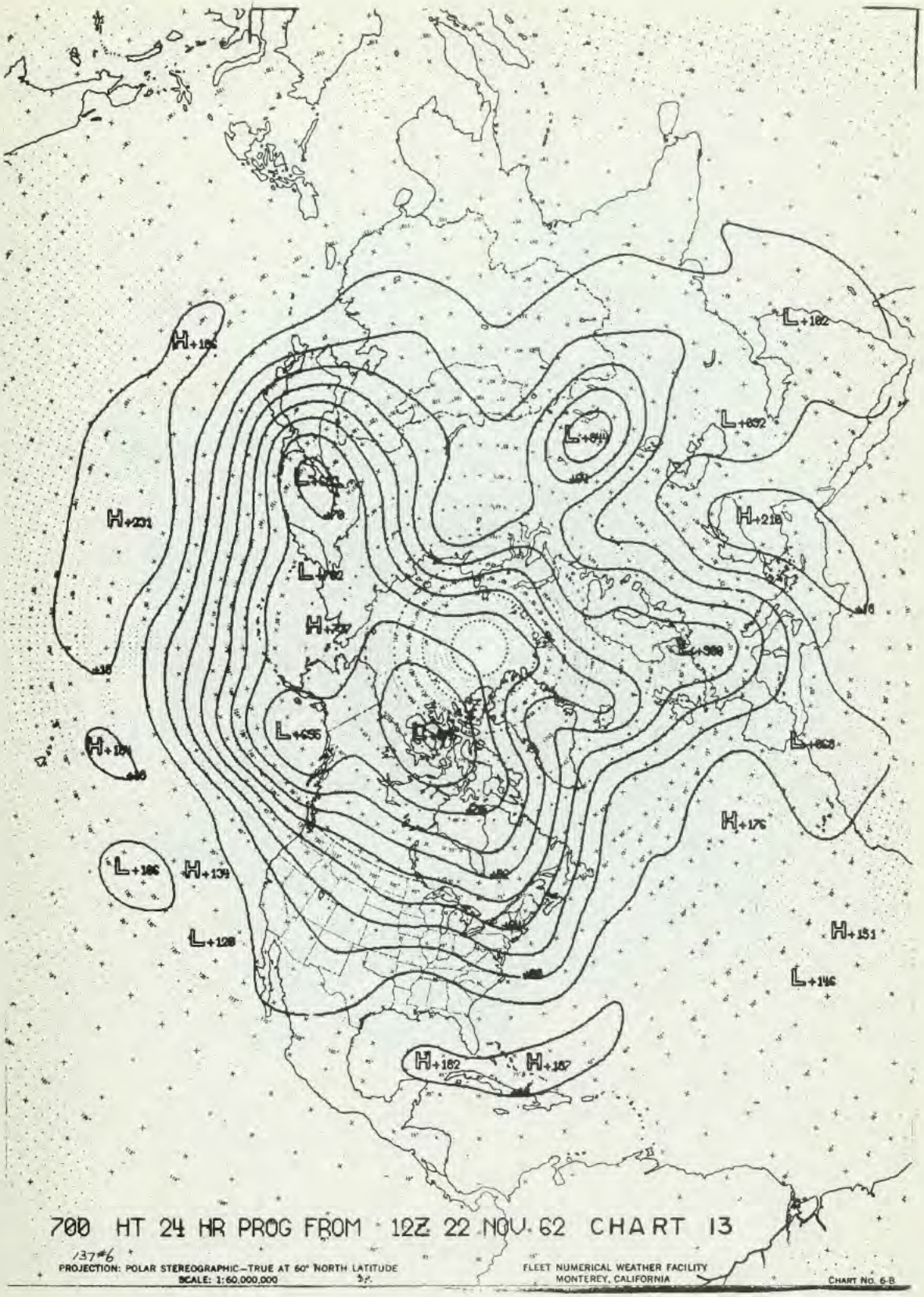
700 HT 24 HR PROG FROM 12Z 22 NOV 62 CHART 13
13746
PROJECTION: POLAR STEREOGRAPHIC—TRUE AT 60° NORTH LATITUDE
SCALE: 1:60,000,000
FLEET NUMERICAL WEATHER FACILITY
MONTEREY, CALIFORNIA
CHART NO. 6-8

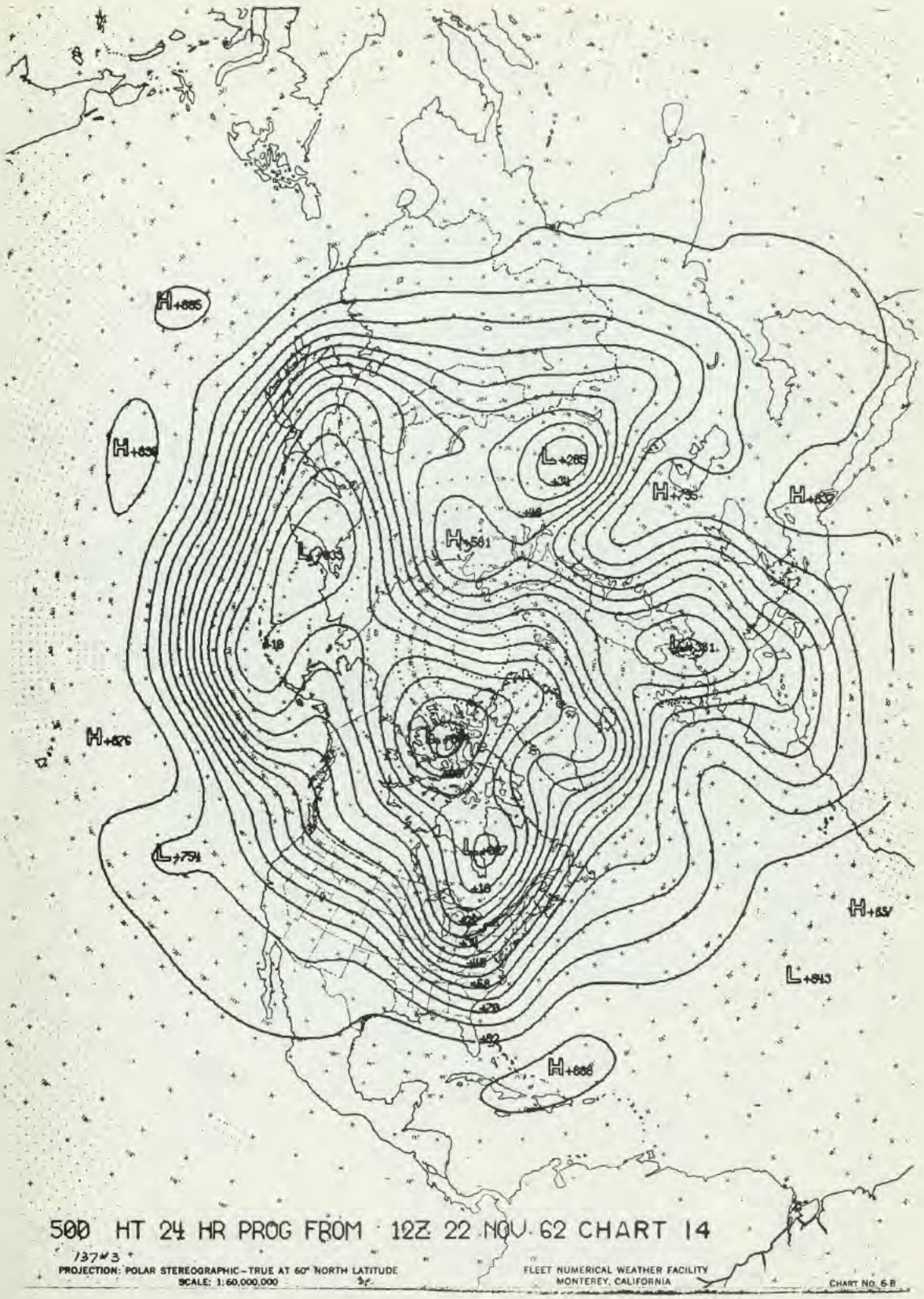
500 HT 24 HR PROG FROM 12Z 22 NOV 62 CHART 14
13743
PROJECTION: POLAR STEREOGRAPHIC – TRUE AT 60° NORTH LATITUDE
SCALE: 1:60,000,000
FLEET NUMERICAL WEATHER FACILITY
MONTEREY, CALIFORNIA
CHART NO. 6-8

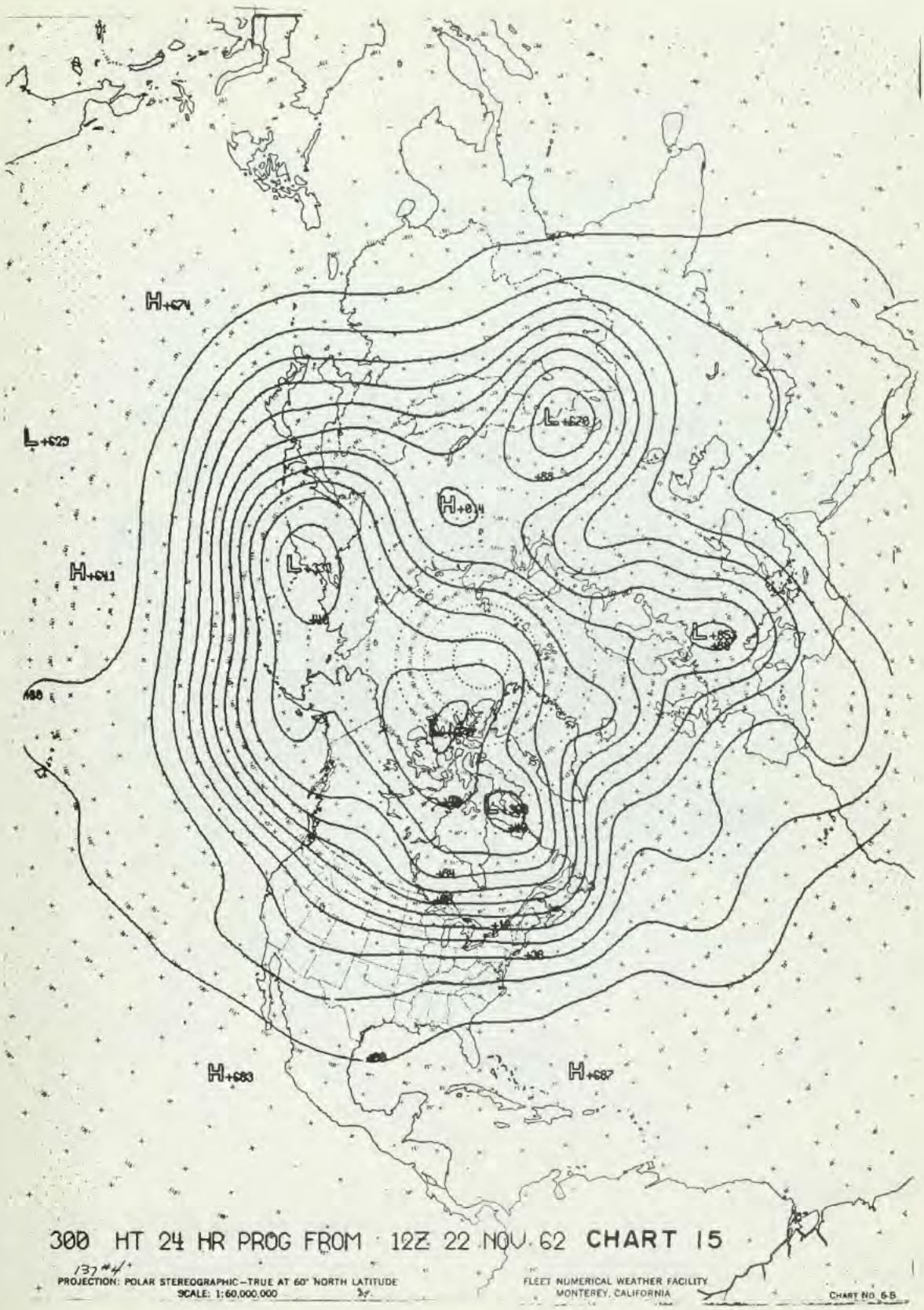

300 HT 24 HR PROG FROM 12Z 22 NOV 62 **CHART 15**

137 #4

PROJECTION: POLAR STEREOGRAPHIC – TRUE AT 60° NORTH LATITUDE
SCALE: 1:60,000,000

FLEET NUMERICAL WEATHER FACILITY
MONTEREY, CALIFORNIA

CHART NO. 6-8

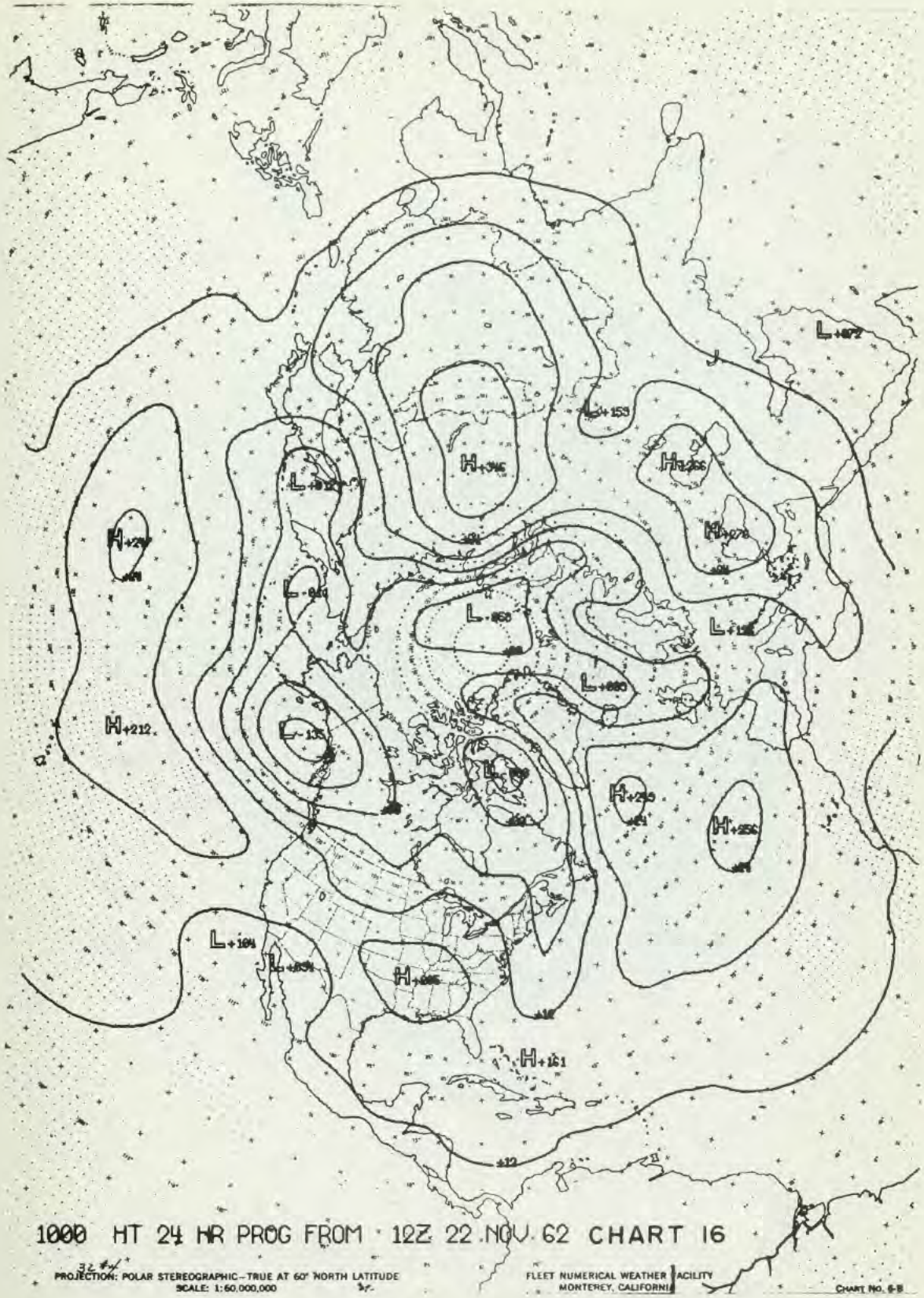
1000 HT 24 HR PROG FROM 12Z 22 NOV 62 CHART 16
PROJECTION: POLAR STEREOGRAPHIC—TRUE AT 60° NORTH LATITUDE
SCALE: 1:60,000,000
FLEET NUMERICAL WEATHER FACILITY
MONTEREY, CALIFORNIA
CHART NO. 6-8

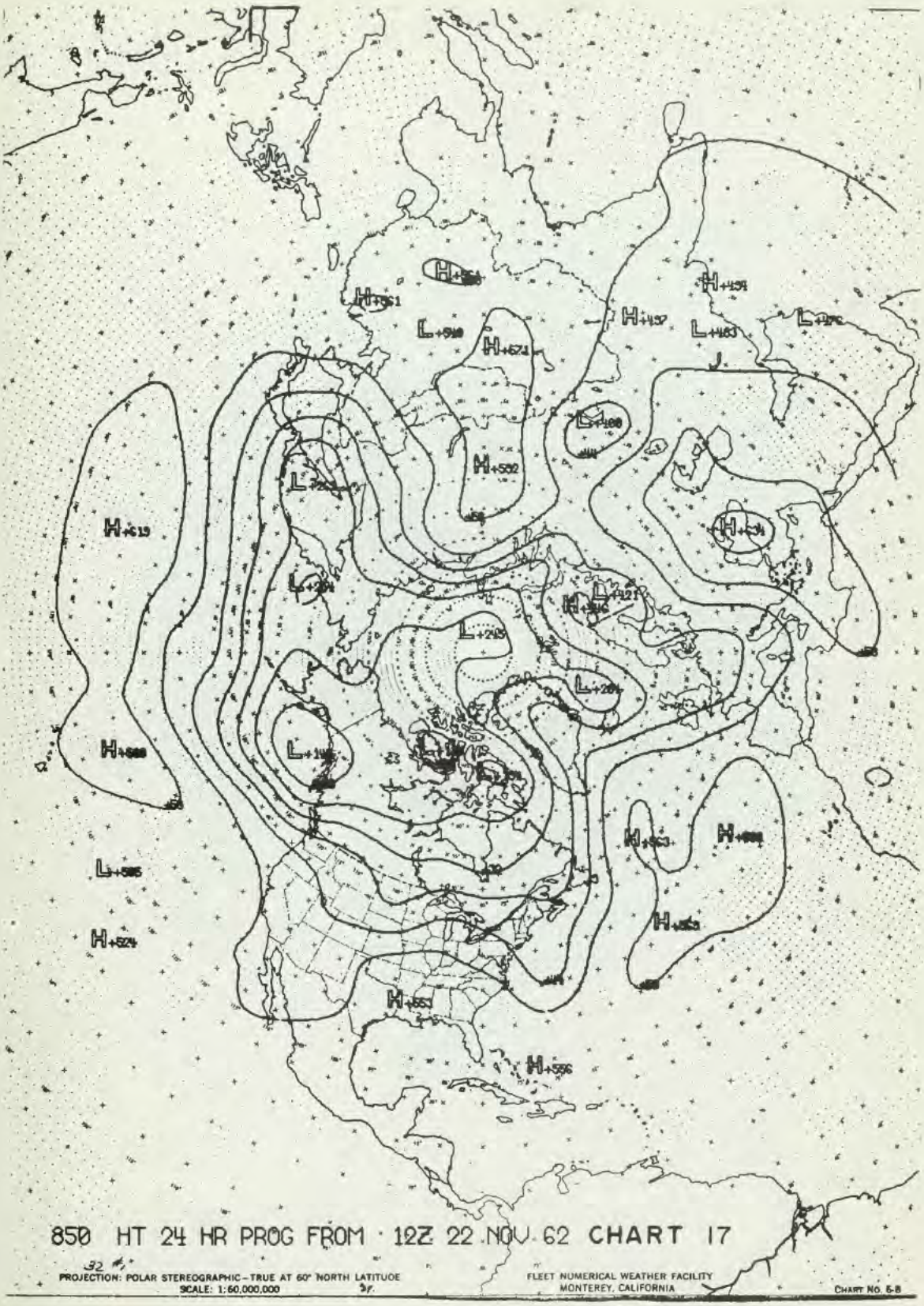
850 HT 24 HR PROG FROM 12Z 22 NOV 62 CHART 17
PROJECTION: POLAR STEREOGRAPHIC – TRUE AT 60° NORTH LATITUDE
SCALE: 1:60,000,000
FLEET NUMERICAL WEATHER FACILITY
MONTEREY, CALIFORNIA
CHART NO. 5-8

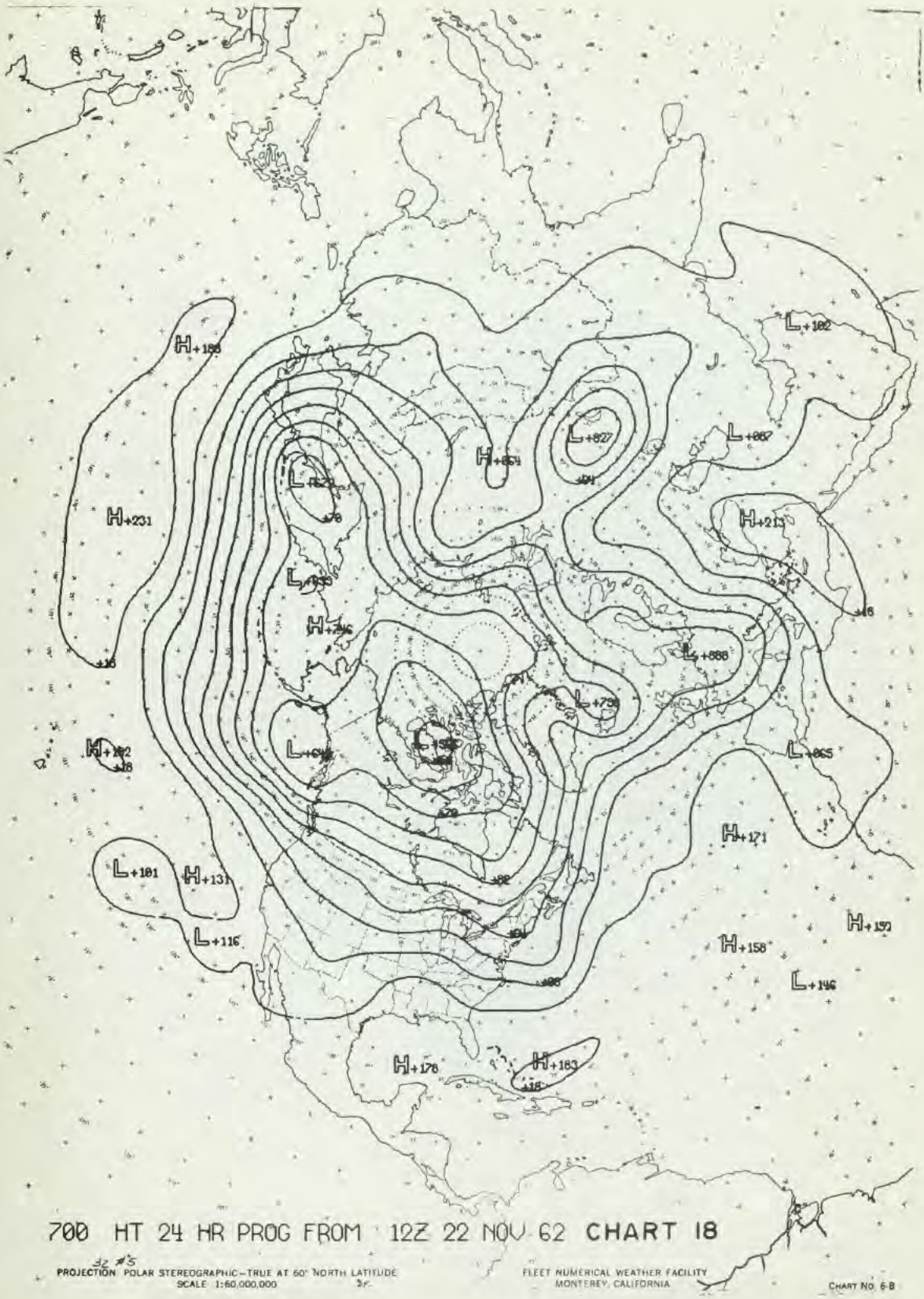

700 HT 24 HR PROG FROM 12Z 22 NOV 62 **CHART 18**

PROJECTION: POLAR STEREOGRAPHIC–TRUE AT 60° NORTH LATITUDE
SCALE: 1:60,000,000

FLEET NUMERICAL WEATHER FACILITY
MONTEREY, CALIFORNIA

CHART NO. 6-8

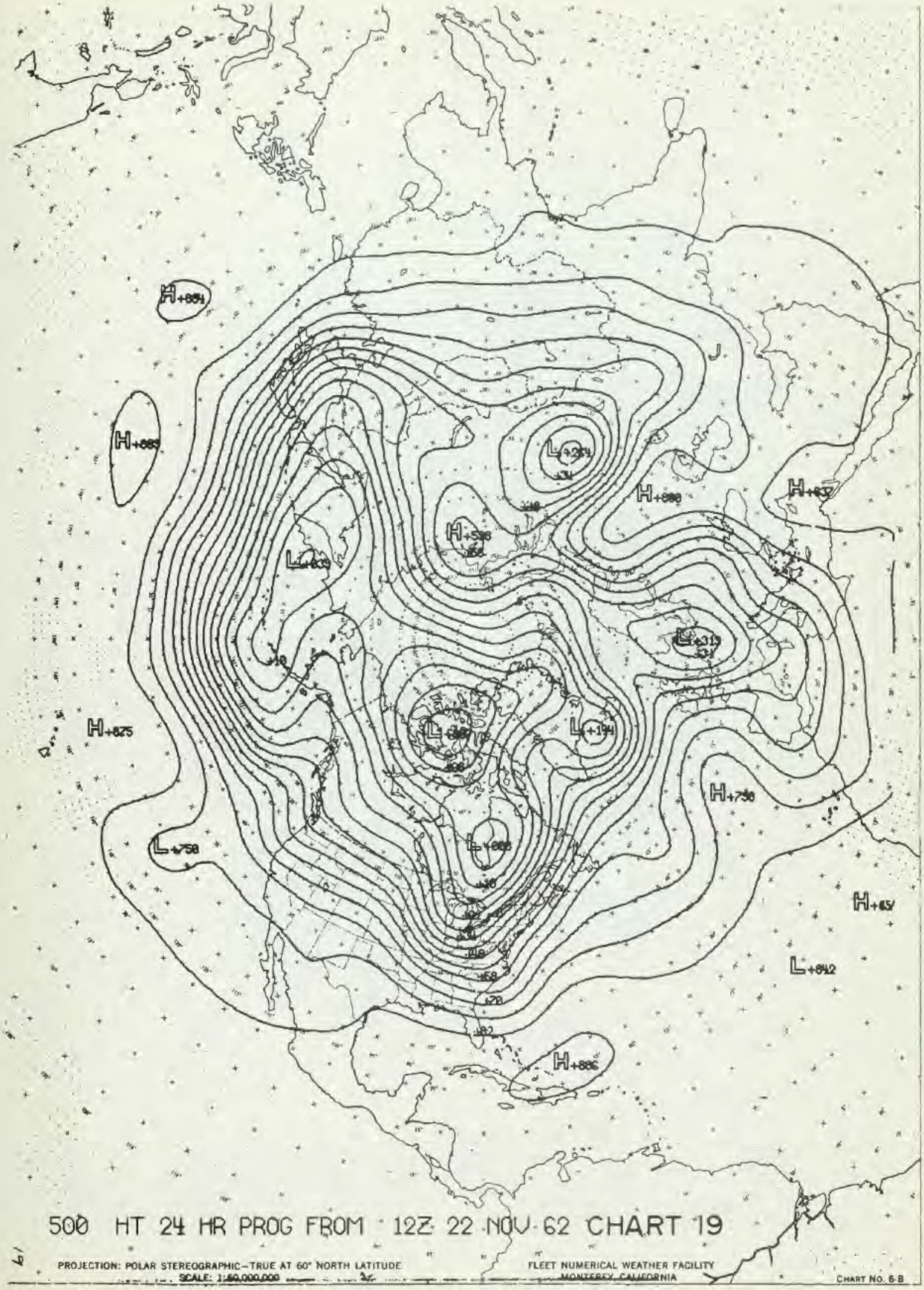
500 HT 24 HR PROG FROM 12Z 22 NOV 62 CHART 19
PROJECTION: POLAR STEREOGRAPHIC – TRUE AT 60° NORTH LATITUDE
SCALE: 1:50,000,000
FLEET NUMERICAL WEATHER FACILITY
MONTEREY, CALIFORNIA
CHART NO. 6-8

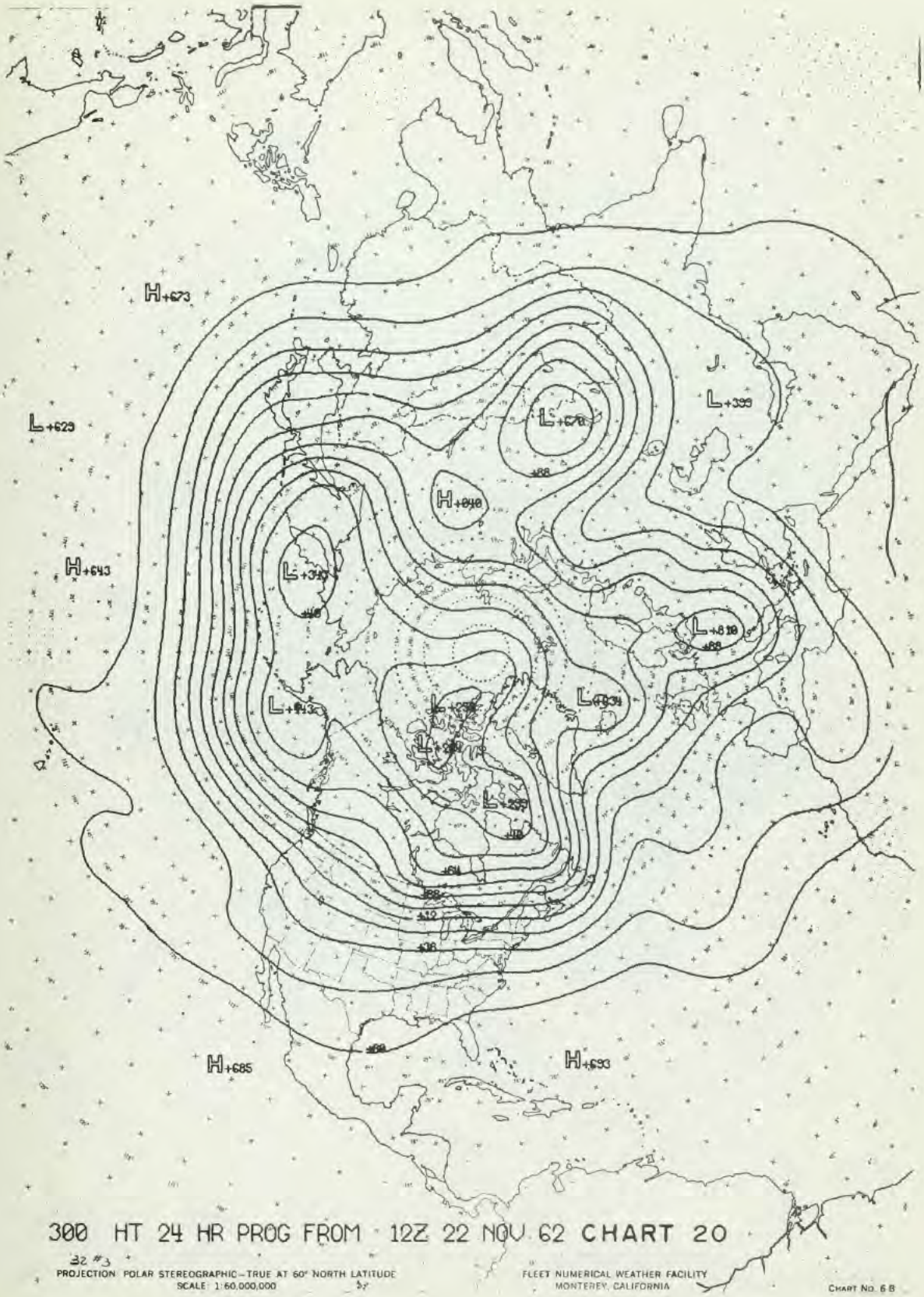

300 HT 24 HR PROG FROM 12Z 22 NOV 62 CHART 20

32 #3

PROJECTION: POLAR STEREOGRAPHIC – TRUE AT 60° NORTH LATITUDE
SCALE: 1:60,000,000

FLEET NUMERICAL WEATHER FACILITY
MONTEREY, CALIFORNIA

CHART NO. 6 B

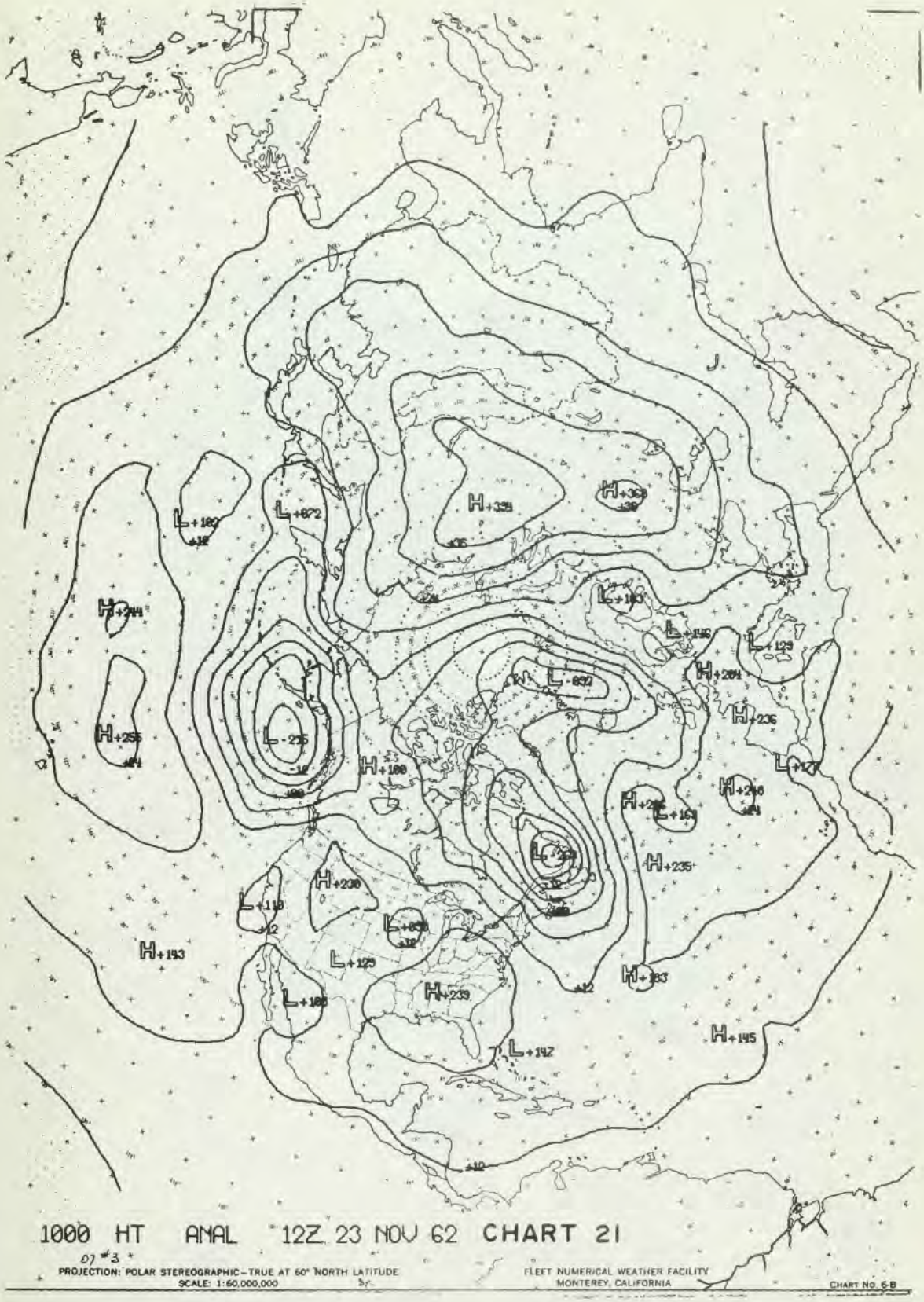
1000 HT ANAL 12Z 23 NOV 62 CHART 21
07 #3
PROJECTION: POLAR STEREOGRAPHIC – TRUE AT 60° NORTH LATITUDE
SCALE: 1:60,000,000
FLEET NUMERICAL WEATHER FACILITY
MONTEREY, CALIFORNIA
CHART NO. 6-8

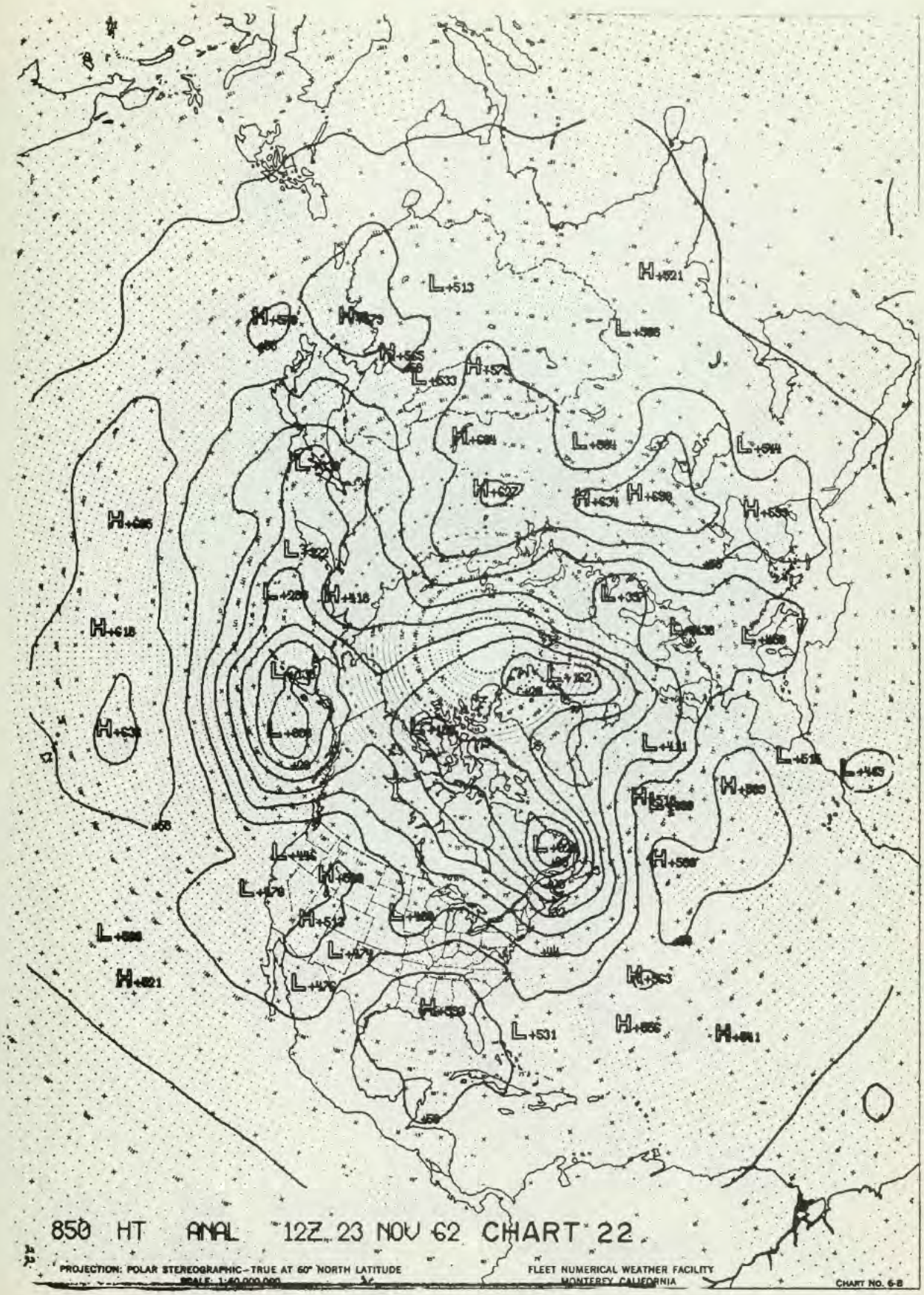
850 HT ANAL 12Z 23 NOV 62 CHART 22
PROJECTION: POLAR STEREOGRAPHIC – TRUE AT 60° NORTH LATITUDE
SCALE: 1:40,000,000
FLEET NUMERICAL WEATHER FACILITY
MONTEREY, CALIFORNIA
CHART NO. 6-8

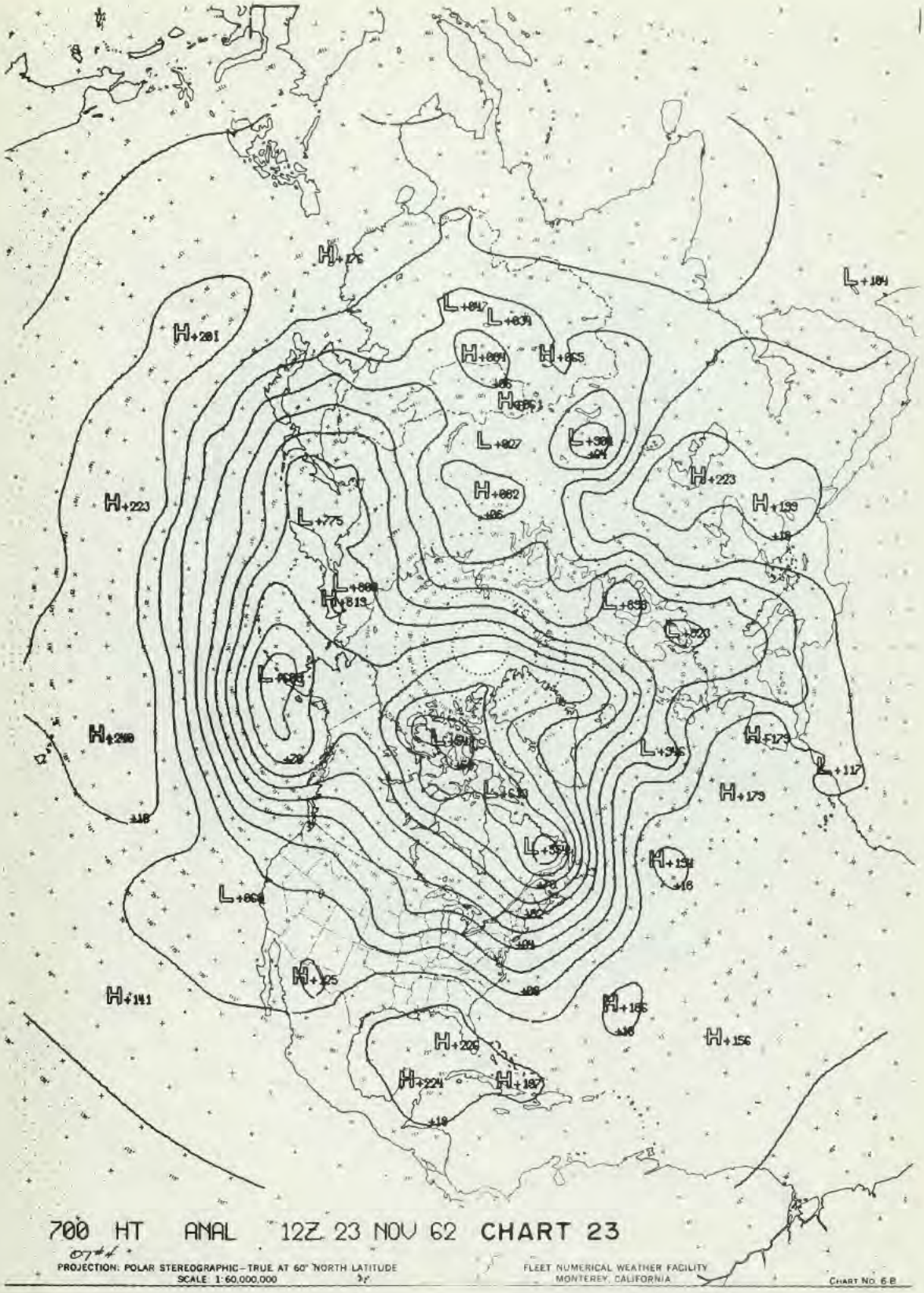
700 HT ANAL 12Z 23 NOV 62 CHART 23
PROJECTION: POLAR STEREOGRAPHIC – TRUE AT 60° NORTH LATITUDE
SCALE 1:60,000,000
FLEET NUMERICAL WEATHER FACILITY
MONTEREY, CALIFORNIA
CHART NO. 6-8

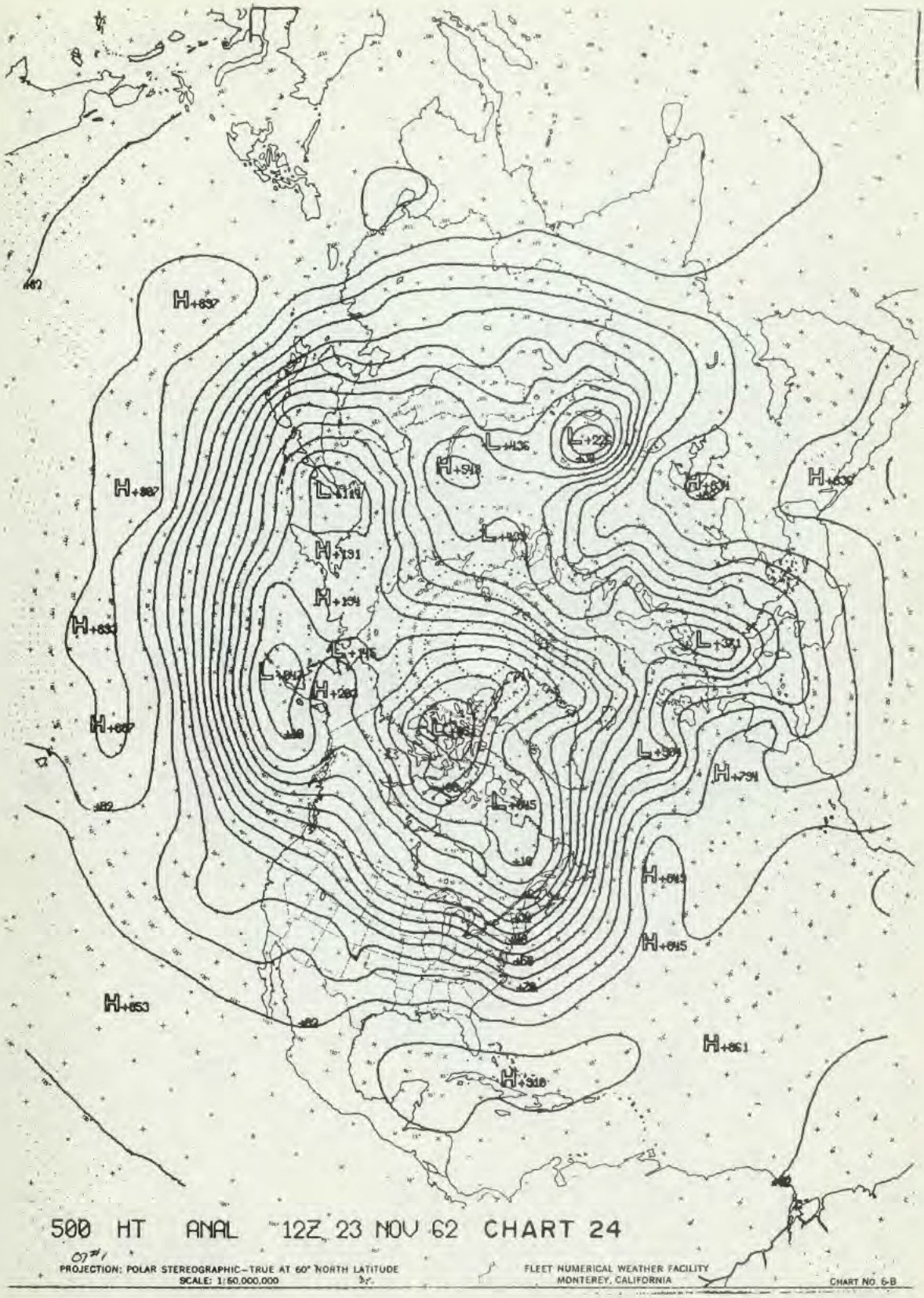
500 HT ANAL 12Z 23 NOV 62 CHART 24
PROJECTION: POLAR STEREOGRAPHIC–TRUE AT 60° NORTH LATITUDE
SCALE: 1:50,000,000
FLEET NUMERICAL WEATHER FACILITY
MONTEREY, CALIFORNIA
CHART NO. 6-B

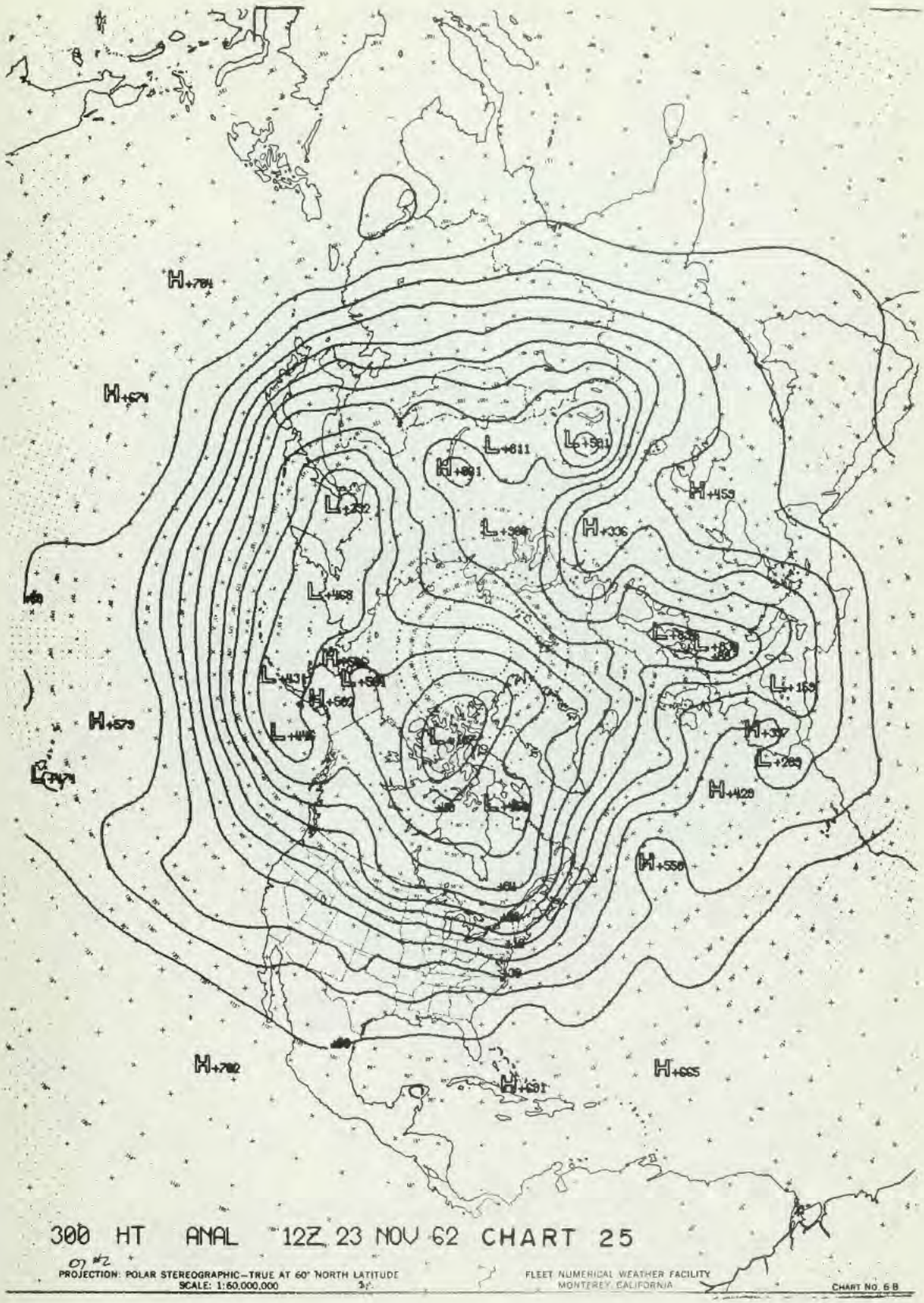
300 HT ANAL 12Z 23 NOV 62 CHART 25
PROJECTION: POLAR STEREOGRAPHIC—TRUE AT 60° NORTH LATITUDE
SCALE: 1:60,000,000
FLEET NUMERICAL WEATHER FACILITY
MONTEREY, CALIFORNIA
CHART NO. 6B

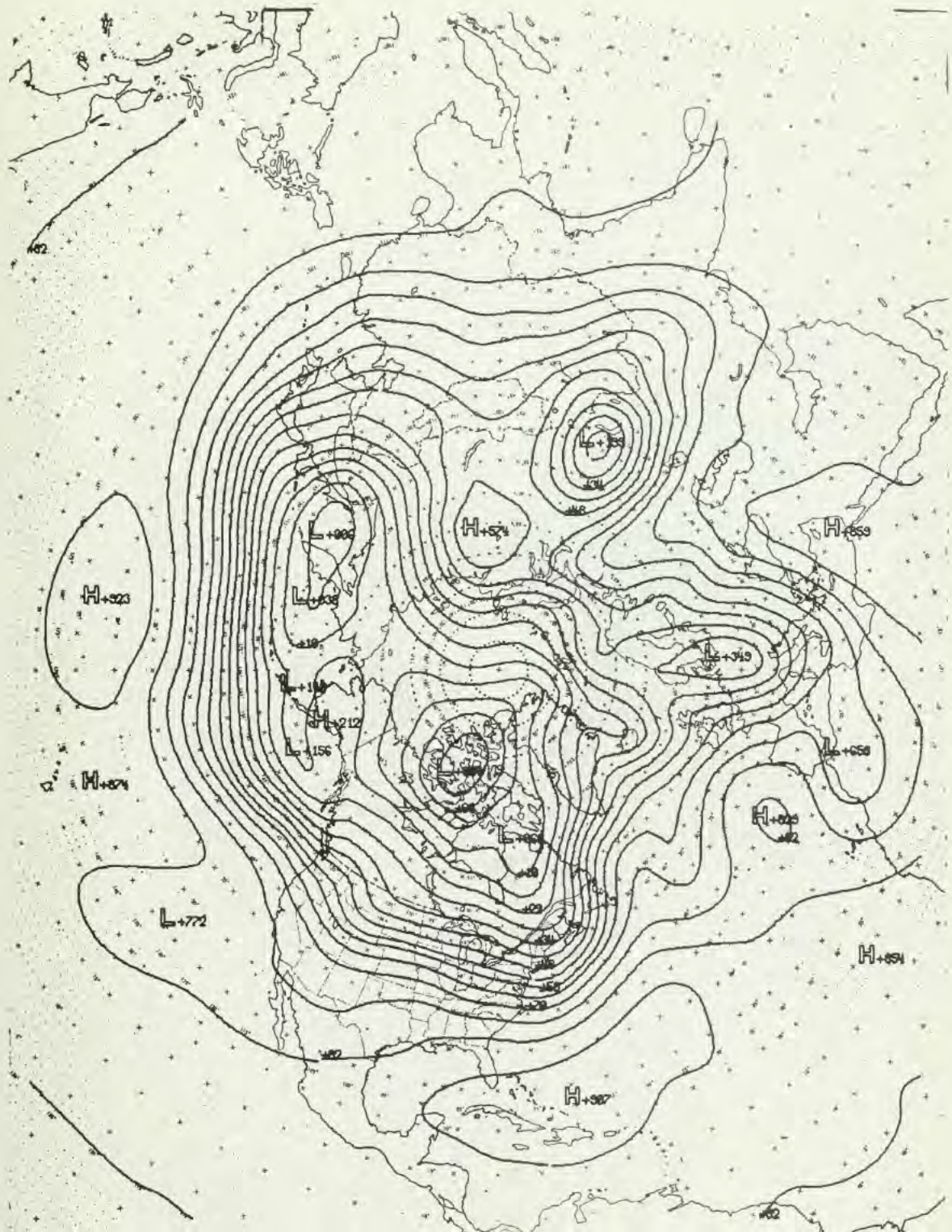

500 HT 24 HR PROG FROM 12Z 22 NOV 62 CHART 26

PROJECTION: POLAR STEREOGRAPHIC–TRUE AT 60° NORTH LATITUDE
SCALE: 1:60,000,000

FLEET NUMERICAL WEATHER FACILITY
MONTEREY, CALIFORNIA

CHART NO. 6-8